Lawrence Berkeley National Laboratory
Recent Work

Title
TOPOLOGICAL BOOTSTRAP THEORY OF HADRONS

Permalink
https://escholarship.org/uc/item/1z40f68d

Authors
Chew, G.F.
Poenaru, V.

Publication Date
1981-05-01

eScholarship.org Powered by the California Digital Library
University of California

LBL-11433 c.2
Preprint

Lawrence Berkeley Laboratory
UNIVERSITY OF CALIFORNIA

Physics, Computer Science & Mathematics Division

Submitted for publication

RECEIVED
AWRENCE
BE ORY
JUN 9 1981
DOCUMENTS SECTION

TOPOLOGICAL BOOTSTRAP THEORY OF HADRONS

G.F. Chew and V. Poénaru

May 1981

Prepared for the U.S. Department of Energy under Contract W-7405-ENG-48

LBL-11433 c.2

DISCLAIMER

This document was prepared as an account of work sponsored by the United States Government. While this document is believed to contain correct information, neither the United States Government nor any agency thereof, nor the Regents of the University of California, nor any of their employees, makes any warranty, express or implied, or assumes any legal responsibility for the accuracy, completeness, or usefulness of any information, apparatus, product, or process disclosed, or represents that its use would not infringe privately owned rights. Reference herein to any specific commercial product, process, or service by its trade name, trademark, manufacturer, or otherwise, does not necessarily constitute or imply its endorsement, recommendation, or favoring by the United States Government or any agency thereof, or the Regents of the University of California. The views and opinions of authors expressed herein do not necessarily state or reflect those of the United States Government or any agency thereof or the Regents of the University of California.

TOPOLOGICAL BOOTSTRAP THEORY OF HADRONS*

G. F. Chew

Lawrence Berkeley Laboratory

and

Department of Physics,
University of California,
Berkeley, California 94720

and

V. Poénaru

Département de Mathématiques
Université de Paris-Sud, 91405, Orsay, France

ABSTRACT

A topological framework is constructed for an S-matrix bootstrap theory of particles. Each component of an S-matrix topological expansion is associated with a pair of intersecting "quantum" and "classical" surfaces whose complexity exhibits an entropy property. The bounded classical surface embeds graphs that carry the direct observables--energy-momentum, spin and electric charge. The closed quantum surface carries a triangulation whose orientations represent internal quantum numbers--which turn out to be baryon number, lepton number and flavor. A form of "color" automatically appears. All strong-interaction components of the expansion are generated through "Landau connected sums" from "zero-entropy" surface pairs--which are self generating. Elementary particles correspond to triangulated areas on the quantum surface; consistency at zero entropy

* This work was supported by the Director, Office of Energy Research, Office of High Energy and Nuclear Physics, Division of High Energy Physics of the U.S. Department of Energy under Contract No. W-7405-ENG-48.

determines allowed hadron disks on quantum spheres together with the associated quantum numbers. Elementary topological hadrons turn out to include mesons, baryons and baryoniums, with quarks appearing as "peripheral triangles" (along the perimeters of hadron disks) whose attachments correspond to a total of 8 flavors as well as spin. Individual quarks do not carry momentum and cannot be hadrons; quark confinement is automatic. Also appearing within hadron disks are "core triangles" that carry baryon number and electric charge but no flavor or spin. Hadron disks have quantum numbers that accord with the lowest-mass physically-observed mesons and baryons. The relation of topological theory to QCD is discussed.

I. INTRODUCTION

The bootstrap idea that S-matrix causality and unitarity might determine all hadron properties is 20 years old--preceding the quark idea. Bootstrap theory developed slowly because of its essential nonlinearity and lost favor when the capabilities of the seemingly-opposite quark approach, eventually formalized within quantum chromodynamics (QCD), became recognized. It was, however, never established that conflict exists between quark and bootstrap ideas. This paper describes a bootstrap theory which explains quarks and their properties on the basis of S-matrix consistency.

Underlying our theory is the notion of causally-connected events in a Poincaré-invariant macroscopic space-time. In other words we accept the analytic S-matrix as described, for example, in the book by Iagolnitzer.[1] We do not require the space-time continuum of local quantum field theory, and we make no a priori assumptions about internal quantum numbers. Our guiding motivation is to satisfy the nonlinear cyclical conditions implied by unitarity and causality: S-matrix connected parts are analytic momentum functions determined by their singularities, while the singularities are determined by products of connected parts, products associated with Landau graphs.[1] Our theory shows how this cycle implies hadron quark structure replete with internal quantum numbers and triality. We predict 8 flavors.

A precondition for the form of bootstrap theory presented in this paper was recognition of the relevance to the S-matrix of combinatorial topology, applied to 2-dimensional surfaces.

An impressive understanding of mesons and meson interactions emerged during the seventies through the application of combinatorial topology to S-matrix causality and unitarity. This program--sometimes called "dual topological unitarization" (DTU)--grew out of Harari-Rosner dual diagrams,[2] and a survey of DTU developments up to 1977 ("classical" DTU) has been given in a Physics Reports review article.[3] The general idea is to associate S-matrix connected parts (amplitudes) with 2-dimensional surfaces that admit a connected-sum operation analogous to matrix multiplication. These surfaces carry complexity indices with an "entropy" property such that in connected sums complexity cannot decrease. Topological expansion of the S-matrix then isolates the nonlinear bootstrap aspect of unitarity-causality at the level of minimum complexity and maximum symmetry--often characterized as the "planar" level. Higher terms in the topological expansion are to be calculated in succession, starting from the planar terms. The theory proposed in the present paper extends DTU but maintains these general ideas.

Our key addition to classical DTU is the "quantum sphere," which houses the "zero-entropy" bootstrap. Quarks and quark properties emerge from demanding consistency of the quantum sphere--the residence of internal (not directly-observable) quantum numbers--with the classical surface carrying energy, momentum, spin and electric charge.

We find it plausible that the low-entropy content of bootstrap theory is complementary to QCD--which postulates colored and flavored quark

and gluon fields with a gauge-invariant interaction. We argue in our conclusion that it is because the validity domain of quantum field theory is "high entropy" that the Lagrangian approach cannot explain the number of colors and flavors. We anticipate that a high entropy limit of our theory will eventually be shown to imply the physical content of perturbative QCD.

Our paper consists of two well-separated parts plus appendices. In the first part (Secs. II-IV) we express classical DTU in a precise form that admits elaborations to describe spin, parity and the possibility of hadrons more complex than mesons. This part closely relates to parallel work by H. P. Stapp[4]; the difference is mainly in our use of Landau graphs and in our emphasis on "Landau connected sums" of graph-carrying classical surfaces. The notion of entropy, including zero entropy, governs both our approach and that of Stapp.

Although it is possible within a topological expansion based on classical surfaces to identify the concept of a zero-entropy bootstrap, the classical surface alone does not provide the means to explore all consistency requirements on internal quantum numbers. The second part of our paper deals with the quantum sphere, which corresponds to a thickening of the boundary of the zero-entropy classical surface. This thickening is needed to achieve a zero-entropy Hilbert space, so that zero-entropy components of the topological expansion become identifiable with elements of an S-matrix. Causality and contraction rules based on particle-bound-state correspondence are then shown to constrain the pattern of internal quantum numbers.

A preliminary summary of the main ideas in the present paper has been published,[5] but subsequent to that publication there became recognized the need for an additional topological feature: singular junction lines connecting "feathers" of a multisheeted classical surface. Introduction of junction lines does not affect the zero-entropy Hilbert space, but there is an impact on the subsequent growth of entropy, which now can be expressed through a thickened Landau graph embellished by "colored" quark lines.

It is natural to extend the topological approach to encompass electromagnetic and weak interactions. The extension to electromagnetism is described in separate papers[6] which propose a topological representation of photons and charged leptons. Leptons and photons are not generated by the zero-entropy bootstrap in the sense of hadrons but there is a common topological framework; the topology of leptons in particular, is similar to that of quarks. A further extension of topological theory to weak interactions is in progress.

II. CLASSICAL DTU

The unitarity-causality properties of an analytic S matrix are expressible through Landau graphs, which stand in one-to-one correspondence with isolated S-matrix singularities (Appendix A). In Ref. 3 (Sec. 5) Landau graphs were given ordered vertices and housed in bounded two-dimensional surfaces which served as basis for an S-matrix topological expansion. We shall refer to such surfaces as "classical" because one of their functions is to keep track of complexity in momentum-energy--continuous particle attributes associated with the Lorentz group that play a central role in classical physics. In Sec. III we shall patchwise orient the classical surface and associate orientation reversal with space inversion (parity); it will then also be possible to describe spin complexity. We begin in the present section, however, with the unpatched surfaces used in Ref. 3 to describe mesons without attention to spin. These surfaces are orientable and inherit global orientation from the ordered-vertex Landau graphs embedded thereon (See Sec. VIII). In Sec. IV a wider class of hadrons, including baryons, will be accommodated by allowing the classical surface to be multisheeted, the sheets being joined together at singular junction lines. In classical DTU for mesons there are no junction lines; the surface is a bonafide 2-dimensional connected manifold with boundary.

Central to classical DTU and to its generalizations is the idea of a topological expansion of "elementary S-matrix" connected parts. The Hilbert space in which the elementary S matrix is defined is based on a notion of "elementary particles". In our theory an elementary

particle is assumed to correspond to a definite physical particle but is not identical therewith. In particular, elementary particles are all stable; their physical counterparts need not be. Anticipating later results, an example is the elementary ρ meson, which will turn out to be one of the basis states for the topological expansion. The physical ρ meson is unstable and its mass is correspondingly a complex number. The elementary ρ mass has no imaginary part, and the real part is only approximately equal to that of the physical ρ meson. All conserved internal quantum numbers are the same, however, as are spin and intrinsic parity. We make the assumption that a unique (not necessarily finite) set of elementary particles can be identified through requirements of S-matrix consistency. Finding this set is the bootstrap problem. The results found in this paper imply a finite but moderately large set of elementary hadrons which all have the same mass; they differ in spin and internal quantum numbers.

The elementary S matrix is assumed to have the same pole structure as the physical S matrix. Thus, even though the elementary ρ has an unphysical mass, we assume the presence in appropriate elementary S-matrix connected parts of a complex pole whose position corresponds to the physical ρ mass. More generally we assume the usual pole, physical-particle correspondence for the elementary S matrix, with the standard factorization property relating pole residues to products of connected parts (Appendix A). All connected parts of the physical S matrix are thus assumed to be obtainable by pole-residue factorization from the elementary S matrix, despite the unphysical basis in which the latter is defined.

Only a finite subset of the infinite collection of poles of the elementary S matrix can be placed in correspondence with elementary particles; other poles correspond to "composite" particles. Again anticipating later results, there will for example be no elementary particle corresponding to the deuteron or to any ordinary atomic nucleus beyond neutron and proton. The structure of our bootstrap theory does not conform to a "nuclear democracy"; there will be a definite and restricted set of elementary particles even though each of the latter is determined by S-matrix consistency and is equivalent to a "bound state" of other elementary particles.

Let us denote by M_{fi} a connected part of the elementary S matrix, the indices i and f designating sets of ingoing and outgoing elementary particles, together with momenta and spins. In classical DTU, as well as in its generalization, one writes an infinite expansion in two indices:

$$M_{fi} = \sum_{\tau,\kappa} {}^{\tau}M_{fi}^{\kappa} \quad . \tag{2.1}$$

We shall refer to M_{fi} as an elementary connected part and to ${}^{\tau}M_{fi}^{\kappa}$ as a topological connected part. The first index τ specifies some surface with embedded graphs, together with some division of the surface boundary into pieces. For example a simple circular boundary component might be divided into n edges--an n-gon. The topological index τ describes the nature of the surface (sphere, torus, etc.), the embedded graphs, and the boundary structure. The second index κ describes an association of the elementary particles in channels f and i with pieces of the boundary. Each particle, for example, might attach to a particular polygon edge.

In classical DTU each τ characterizes an orientable and bounded 2-dimensional connected surface. The index τ specifies the surface genus and boundary structure--the latter corresponding to removing a collection of disks from a closed surface. The perimeter of each removed disk is divided into pieces, and the order index κ associates each such piece to one of the elementary particles in the collection i, f. Embedded on the surface is a single-vertex Landau graph (Appendix A) with one external arc for each particle, each graph "end" lying on a boundary piece. Assigning an elementary particle to a boundary piece is equivalent to attaching this particle's energy-momentum to the corresponding external Landau arc. The contraction rules of Appendix A imply that in classical DTU the Landau graph is a redundant feature of the topology, but it will not be redundant in our extension of classical DTU in Secs. III and IV.

Consider the elementary-particle reaction AB → CD described by the 4-arc vertex of Fig. 1. One of the terms (τ,κ) in the topological expansion of the elementary connected part for this reaction would correspond to the 4-edge disk of Fig. 2, together with embedded single-vertex Landau graph. Notice that the arcs incident on a Landau vertex automatically acquire a cyclic order as soon as the Landau graph is embedded on a 2-dimensional surface. Reference 3 adopted a convention of always understanding this order to be "clockwise". Hence the circular arrow in Fig. 2.

An example of a different term in the topological expansion of the same reaction amplitude is shown in Fig. 3. Here the boundary

consists of 2 disconnected components* each of which is a 2-gon. The particles A and B belong to one boundary component while C and D belong to the other. Note the extra closed loop in the Landau graph--that cannot be contracted. It is the accommodation of this loop that requires two disconnected boundary components. We have here an illustration of how complexity of graph correlates with complexity of surface.

A third example is given in Fig. 4, where the surface is toroidal but the boundary is connected (a single boundary component)--quadrilateral as in Fig. 2 even though we have been forced in drawing Fig. 4 to curve some of the edges. The genus of the surface in Figs. 2 and 3 is zero while that of Fig. 4 is 1. The complete topological expansion requires classical surfaces of indefinitely large genus and the number of disconnected boundary components may be as large as the number of involved particles. All possible cyclic sequences of particles on boundaries must be included.

Landau graphs, as originally introduced in S-matrix theory to describe connected-part singularities (Appendix I), always have more than one vertex and do not have ordered vertices. A nonordered Landau graph L, such as that of Fig. 5(a) corresponds to a discontinuity formula schematically expressible as

$$\text{disc}_L \; M_{fi} = \int dp_L \; M_{\ell m} \times M_{np} \times \ldots \qquad (2.2)$$

* This 2- boundary surface is a cylinder.

where the integration is over the phase space of all intermediate elementary particles--each corresponding to an internal arc of the graph. Because of the difference between physical particles and elementary particles, Eq. (2.2) acquires consistent meaning when applied to elementary connected parts only after a topological expansion has been made of each connected part appearing therein. We have emphasized that the singularities of each M_{fi} (without expansion) correspond to intermediate physical particles, but the intermediate particles of Eq. (2.2) are elementary. This conflict we assume to be reconciled by mass renormalization. The singularities of individual topological connected parts ${}^{\tau}M^{K}_{fi}$ correspond to elementary particles associated with internal arcs of ordered-vertex Landau graphs. (See Formula (2.3) below.) But because the topological expansion Eq. (2.1) is infinite it is possible to assume that the expansion diverges at isolated points in the complex momentum Riemann surface so as to remove elementary unphysical singularities present in individual expansion components and to replace them by physical singularities.

Although the foregoing phenomenon might sound unreasonable, it is in fact familiar in physical theories which achieve unitarity though infinite expansions. Mass renormalization is by now understood in a variety of S-matrix models as well as in Lagrangian field theory. While recognizing the importance for the future of achieving a firm general basis for this aspect of bootstrap theory, we believe it reasonable here to proceed by accepting on faith the implicit assumption of classical DTU[3] that mass renormalization will occur through the above mechanism.

The attribution of formal meaning via the topological expansion to the discontinuity formula (2.2) associates the notion of Landau connected sum with an ordered multivertex Landau graph. Consider the 2-vertex nonordered Landau graph of Fig. 5(a) and associate this with a product of two elementary connected parts, as on the right-hand side of Eq.(2.2). Topological expansion of each of the two connected parts leads to a sum of products

$$\mathrm{disc}_L\, M_{fi} = \sum_{\substack{\tau',\kappa' \\ \tau'',\kappa''}} \int dp_L\, {}^{\tau'}M_{\ell m}^{\kappa'} \times {}^{\tau''}M_{np}^{\kappa''}, \qquad (2.3)$$

each product being associable with a 2-vertex ordered Landau graph L such as that of Fig. 5(b). Each vertex here corresponds to a topological connected part, so the incident arcs lie in a definite cyclic sequence. This ordered graph belongs to a Landau connected sum, denoted by

$$(\tau',\kappa') \underset{L}{\#} (\tau'',\kappa'') = (\tau,\kappa) \qquad (2.4)$$

or, more compactly, if $\Sigma' \equiv (\tau',\kappa')$ and $\Sigma'' \equiv (\tau'',\kappa'')$,

$$\Sigma' \underset{L}{\#} \Sigma'' = \Sigma, \qquad (2.4')$$

a notion defined precisely in Appendix B. There is a joining of boundary edge segments belonging to intermediate elementary particles so as to achieve a unique new surface whose boundary edge segments correspond to external elementary particles. The two ingredient surface orientations inherited from the single-vertex Landau graphs

are to match so that the two-vertex graph on the new surface has a coherent orientation (say clockwise). Contraction of this graph to a single-vertex graph (Appendix A) then completes the specification of (τ,κ)*.

In the example of Fig. 5(b) a connected sum is formed from two single-boundary, zero-genus classical surfaces, the boundary of each having 5 pieces. There is a joining of corresponding boundary segments on the two surfaces--belonging to intermediate elementary particles E, F, G--to achieve a new surface whose boundary only includes particles A, B, C, D. The new surface in fact is that of Fig 4., where the single-vertex Landau graph is a contraction (Appendix A) of the 2-vertex ordered graph of Fig. 5(b).

Suppose now that we topologically expand the left-hand side of an equation like Eq. (2.3) and associate with each (τ,κ) those terms on the right-hand side for which the associated connected sum is (τ,κ). We then find

$$\mathrm{disc}_L\, {}^{\tau}M_{fi}^{\kappa} = \sum_{\substack{\tau',\kappa' \\ \tau'',\kappa'' \\ \cdots}} \int dp_L\, {}^{\tau'}M_{\ell m}^{\kappa'} \times {}^{\tau''}M_{np}^{\kappa''} \cdots \qquad (2.5)$$

where the sum is restricted by $(\tau',\kappa') \# (\tau'',\kappa'') \# \ldots = (\tau,\kappa)$.

Equation (2.5) implies that each topological connected part ${}^{\tau}M_{fi}^{\kappa}$ is an analytic function of particle momenta with isolated singularities corresponding to multivertex ordered Landau graphs that contract to the single-vertex graph belonging to (τ,κ). Reference 3 presents

---

* The elaboration of classical DTU discussed in later sections will require modification of this Landau-graph contraction rule.

a variety of examples showing how Formula (2.5) implies different singularity structure for different values of (τ,κ). Each individual topological connected part ${}^{\tau}M_{fi}^{\kappa}$ possesses only a small subset of the singularity collection present in all the components building M_{fi}.

To complete a meaning for the topological expansion it is necessary to assume that discontinuity formulas such as (2.5) together with Cauchy-Riemann formulas (dispersion relations), provide a basis for calculating topological connected parts. The scheme by which the calculation is supposed to proceed depends on notions of <u>entropy</u> and <u>zero entropy</u>. The Landau connected sum of classical surfaces has the property that if the genuses of the ingredient surfaces are g', g",..., and the genus of the resultant is g, then

$$g \geqslant g' + g'' + \ldots \tag{2.6}$$

We refer to such a property that surface complexity can only increase through surface addition as "entropy". Its importance for the S matrix was first noted by Veneziano.[7] Entropy rules also apply to boundary structure (Appendix B). For example, if the number of boundary components on the surface resulting from a Landau connected sum is smaller than the maximum number on any ingredient surface, there must be an increase in resultant genus over the sum of ingredient genuses.[8]

A consequence of such entropy rules is the possibility of identifying a minimal subset of <u>zero-entropy</u> topological connected parts, whose discontinuities are built entirely from products of zero-entropy connected parts. In classical DTU the zero-entropy

subset consists of all τ where the surface is a disk--with zero genus and a single boundary component--commonly characterized as "planar". (In our generalizations of classical DTU, the adjective "planar" will not be sufficient to describe zero entropy.) That is, any discontinuity of a planar connected part is a product of planar connected parts. Classical DTU makes the assumption, to which we shall adhere in our generalizations, that zero-entropy connected parts may be calculated <u>first</u>, without having to calculate any connected parts outside this subset.

A second assumption, also to be maintained, is that all strong-interaction components of the topological expansion (2.1) correspond to surfaces that can be formed by successive connected sums of zero-entropy surfaces. A feature of our theory is that any higher component in the topological expansion may be calculated through <u>linear</u> equations, given components of lower entropy. This feature accords with the fact that the complexity of any ingredient surface in a Landau connected sum cannot exceed that of the resultant. For example, the inequality (2.6) means that the only genus of a resultant surface which can occur more than once among ingredient surfaces is zero genus; discontinuity formulas for a topological connected part of genus $g \neq 0$ may contain at most a <u>single</u> factor corresponding to a genus-g connected part. All other factors must have smaller genus, so the calculation may proceed through a linear equation.

In contrast, the calculation of zero-entropy connected parts is nonlinear and herein lies the bootstrap potential. Arbitrary assignment of elementary particles is presumed not to be possible: the

basis for the topological expansion must be chosen so as to permit satisfaction of the nonlinear zero-entropy equations. It is shown in Ref. 3 how these equations imply a zero-entropy "ordered S matrix". We do not at this point repeat the reasoning since we shall later consider in detail the ordered S matrix after adding the "quantum surface", a notion absent from classical DTU. Suffice it here to say that unitarity and causality properties of the physical S matrix imply corresponding properties in a zero-entropy Hilbert space of elementary particle channels.

Every elementary hadron is at the same time a composite "bound state" built from other elementary hadrons. This idea is made precise by topological contraction rules. For elementary mesons in classical DTU the rule means that a connected boundary interval belonging to several mesons can be uniquely contracted to a smaller boundary piece belonging to a single meson. The notion of multi-particle boundary-piece contraction to a single-particle boundary piece is the essential element in distinguishing strong from electroweak interactions.[14]

The classical-DTU contraction rule is often expressed with the aid of graphs invented by Harari and Rosner.[2] Every meson boundary piece is divided into two subpieces, and the complete set of subpieces building a zero-entropy boundary is grouped into adjacent mated subpiece pairs, where the two members of a pair belong to different mesons. An arc can be drawn on the classical surface connecting the two members of a mated pair, as shown in Fig. 6 (which corresponds to Fig. 2), and the collection of mate-connecting arcs is the Harari-Rosner (HR) graph. Figure 6 also shows how orientations may be

attached to HR arcs so as to agree with the vertex orientation in the Landau graph. Henceforth we shall refer to this global orientation of the surface as HR orientation.

To contract a multimeson boundary interval into a single-meson interval one removes all mated pairs and erases the corresponding HR arcs. Topologically this contraction may be described as a degenerate connected sum, as seen in the example of Fig.7, where adjacent mesons C and D contract to a single meson. Notice how the contraction produces and erases a closed HR loop; such closed loop production and erasure is also a typical feature of zero-entropy Landau connected sums.

It should be remarked (see Fig. 6*) that in classical DTU the Landau graph and the HR graph give the same information, although such will no longer be the case after the classical surface is generalized to accommodate elementary hadrons other than mesons. As discussed in Appendix B, ordering of Landau-graph vertices allows a unique 2-dimensional thickening of the Landau graph; the Harari-Rosner graph lies along the boundary of the thickened Landau graph.**

---

* The orientation of the Landau arcs is not significant, since analytic continuation in particle energy (Appendix D) changes ingoing particles to outgoing antiparticles.

** Chapter 5 of Ref. 3 describes a rule which allows the genus and boundary structure of the classical-DTU surface to be deduced entirely from the vertex-ordered Landau graph. Section VIII below gives further discussion of thickened Landau graphs.

We are here encountering a characteristic feature of topological bootstrap theory, where a single structure may simultaneously play different roles. HR graphs reflect singularity structure in continuous energy-momentum variables, inasmuch as they conform to Landau graphs, but in describing zero-entropy contraction rules they also control the structure of dependence on discrete "internal" variables. Weissmann[9] was able to show for classical DTU that additively-conserved internal quantum numbers can consistently be introduced into the zero-entropy topological S matrix only as indices attached to HR arcs,* to be matched in connected sums. A glance at Fig. 6 then allows the conclusion that, so far as flavor is concerned, mesons necessarily act like quark-antiquark combinations. Below, by slightly enlarging classical DTU, we shall find that zero-entropy spin dependence conforms to this same pattern. Thus HR arcs, with respect both to flavor and to spin, may be described as "quark lines"; in this sense the zero-entropy classical-DTU bootstrap has explained the quark structure of mesons.

---

* The original discovery of HR graphs[2] rested on attachment of flavor indices to HR arcs.

III. CLASSICAL PATCHES AND SPIN

To describe spin and parity a patchwise orientation (Appendix C), that induces an orientation of patch boundaries, is assigned to the classical surface. A zero-entropy surface is a single patch; if the patch orientation agrees with the HR orientation we characterize the zero-entropy topology as "ortho", if the two orientations disagree the adjective "para" will be employed. Stapp[4] has shown how the ortho-para distinction allows elementary-particle spin to be described through 2-valued indices belonging to $(0, \frac{1}{2})$ or $(\frac{1}{2}, 0)$ spinor representations of the Lorentz group, one index for each quark interval on the classical-surface boundary. The spin of an elementary meson is then carried by a pair of such indices. In Appendix D we give the precise form of Stapp's zero-entropy topological connected-part dependence on spin indices, which loosely may be characterized as a maintenance of spin value along an HR arc. That is, at zero entropy if the nature of the spinor indices is correctly chosen, one may think of a definite spin value $(\pm \frac{1}{2})$ as being attached to each HR arc.

The Stapp zero-entropy spin structure furthermore corresponds to associating the parity operation with reversal of classical-surface patch orientation (Appendix D). Applying space inversion to an ortho component of the topological expansion produces a result equal to the corresponding para component.* Since zero-entropy components always occur in

---

* Separate zero-entropy components of the topological expansion are not parity invariant.

symmetrical ortho-para pairs and since higher strong-interaction expansion components are all generated from zero entropy, it follows that parity is a strong-interaction symmetry. Stapp also has shown that charge conjugation corresponds to simultaneous reversal of patch and HR orientation--another symmetry operation.[4] The elaboration of topological theory to describe hadrons more complex than mesons will maintain strong-interaction C and P symmetry by continuing to employ both patch and HR orientations (Appendix D).

From the foregoing it follows that the spectrum of elementary mesons is characterized by spin quartets, each a triplet (S = 1) degenerate with a singlet (S = 0). The ortho-para doubling of the topology means that each elementary meson appears twice in the spectrum of zero-entropy poles. An ortho plus para (0 + P) zero-entropy ground state pole turns out to have negative intrinsic parity while an ortho minus para (0 - P) has positive intrinsic parity. It is shown by Stapp[7] that the superposition in Formula (2.1) (also Formula (3.1) below) eliminates ground-state poles corresponding to 0 - P, so elementary mesons possess odd intrinsic parity. The spin-parity content of the elementary DTU meson spectrum is thus identical to that of ground states in naive quark models; at the same time ortho-para topological doubling is essential for completeness and consistency.

A Landau connected sum of two zero-entropy surfaces, one ortho and one para, leads to a 2-patched surface with a transition arc separating an ortho patch from a para patch. Further connected sums may add further "classical patches" and, correspondingly, further transition arcs. Patches cannot disappear; the number of patches

resulting from a connected sum is never less than the maximum number in any ingredient surface.* This entropy property allows the consistent demand of no transition arcs on zero-entropy surfaces.

The rules of Landau connected sums imply that, for strong-interaction topologies, transition arcs reaching the boundary do so only at points separating one hadron piece from the next. The boundary direction induced by the adjacent patch can reverse only at such points, being continuous thoughout any particle interval;** in any strong-intersection topological connected part each elementary hadron is attached unambiguously either to an ortho or to a para patch.

The Stapp spin rule[4] implies that after making a Landau connected sum, Landau-graph contractions are to be made only within individual classical patches. There is a single Landau vertex inside each patch, and the number of arcs connecting two vertices in different patches is a significant aspect of the topology τ; the (external) spin dependence of a topological connected part is sensitive to the number of patch-connecting internal Landau arcs.

What is the connection between the unpatched classical DTU of Sec. II and the ortho-para extension? At zero entropy there is no difference; the unpatched problem is duplicated twice. Suppose we

---

* The number n^c of closed transition arcs (loops not touching the boundary) exhibits a stronger entropy rule: In a connected sum $\Sigma = \Sigma_1 \# \Sigma_2$, $n^c \geq n_1^c + n_2^c$.

** This property changes when electromagnetism is introduced.[14]

generally designate by τ_c the content of τ apart from classical patches and Landau graphs; in other words τ_c has the content described in Sec. II. The full set of topologies τ is divided into subsets each labeled by τ_c. Then, if a "fully patched" topological connected part is defined as

$$ {}^{\tau_c}M_{fi}^{K} \equiv \sum_{\tau \in \tau_c} {}^{\tau}M_{fi}^{K} , \tag{3.1} $$

Stapp's considerations show that the discontinuity formulas for ${}^{\tau_c}M_{fi}^{K}$ have the same form as in unpatched classical DTU, with all poles corresponding to 0 + P.

There is, however, a subtle difference between a theory that starts with classical patches and then sums over them and a theory that ignores this topological degree of freedom. The difference lies in the basis--in the "elementary" particles to which the indices i,f refer. For example, zero-entropy elementary mesons exhibit singlet-triplet (e.g.,ρ-π) degeneracy. There is no reason to expect such degeneracy in unpatched classical DTU. Correspondingly if one considers the first few terms in Formula(3.1)... one patch plus 2 patches plus 3 patches, etc. ... for a planar connected part, one finds that with more than a single patch Stapp's spin rule breaks the singlet-triplet degeneracy.[9] The infinite series building a fully-patched planar connected part shifts pole positions by the mass-renormalization mechanism discussed in Sec. II and there is no reason for these shifts to be equal for spin 0 and spin 1. At the same time the <u>basis</u> for ${}^{\tau_c}M_{fi}^{K}$ remains zero-entropy. In unpatched classical DTU the basis would correspond to the poles of the planar

S matrix and there would be no immediate way to know the spin and parity values for the basis states.* Spin and parity remain outside the bootstrap framework in unpatched classical DTU.

---

* Calculations in unpatched classical DTU have taken the meson spins and parities as given by experiment.[3]

IV. FEATHERED CLASSICAL SURFACES, GLITCHES AND THE BELT GRAPH

The classical surfaces described in Secs. II and III are inadequate for the full representation of hadrons more complex than mesons. Although the Landau graph can be accommodated, the topology is too simple to represent spin and internal quantum numbers for elementary particles whose structure goes beyond 2 quarks. It was suggested some years ago by several independent authors[10] that "feathered" surfaces might be appropriate; in this section we attach to the topological index τ a significance belonging to such an object.* A complete and precise definition of a feathered τ depends, as for the τ of unfeathered classical DTU, on a notion of zero entropy and on the way that classical surfaces are inductively constructed from zero entropy. Let us commence forthwith the gradual, somewhat circular, defining process.

---

* An earlier version of our theory, described in an unpublished preprint (G. F. Chew and V. Poenaru LBL-9768, Sept. 1979) and summarized in Ref. 5, attempted to describe complex hadrons without feathered surfaces. It was pointed out to us by J. Finkelstein and J. Uschersohn, (Berkeley, 1980) that inconsistencies develop at nonzero entropy if Σ_C is unfeathered. The form of the quantum surface, Σ_Q, described here in Sec. V is unchanged from the earlier version of the theory. Furthermore, because at zero entropy all the action is on a single sheet of Σ_C (see below), it turns out that the topology of zero entropy remains unchanged for the entire surface pair (Σ_Q, Σ_C).

A feathered classical surface Σ_C is a 2-dimensional object which locally is like a bounded smooth surface except for a finite number of "junction lines". A junction line can be either a segment or a circle, and along such a line three pieces of smooth surface meet. Why three? After introduction of the quantum surface there will emerge reasons for the magic quality of "threeness" in the achievement of overall consistency. Temporarily, the reader may be content to anticipate that a 3-feathered classical surface will correspond to the 3 quarks within a baryon. We shall find, however, that 3-feathered surfaces can accommodate elementary particles with more than 3 quarks and also with less. In Fig. 8 we show a junction-line segment,* with 3 adjoining pieces of smooth surface.

When Σ_C is disconnected along the junction lines it becomes decomposed into a number of connected smooth surfaces which we call sheets. Each sheet is orientable and patchwise oriented--the kind of object described in Sec. III. Each sheet furthermore carries a coherent HR orientation which, as in classical DTU, can be associated with ordered Landau vertices on the sheet (see below) or, alternatively, with HR arcs along the boundary (see Fig. 8).

The boundary of the full multisheeted classical surface Σ_C is a closed cubic graph (3 arcs incident on each nontrivial vertex)

---

* The 3 pieces of smooth surface can interconnect in a nontrivial fashion.

which we call the belt and denote by $\partial\Sigma_C$.* If S is one of the sheets of Σ_C, the boundary of S consists of belt segments ($S\cap\partial\Sigma_C$) and junction lines. Along $S\cap\partial\Sigma_C$ there are HR arcs, as in Fig. 8, which provide HR orientation. Attaching the HR orientation to the sheet boundary orients any junction line along the boundary. We require that all 3 sheets meeting along a junction line J give the same HR orientation to J.**

Each HR arc carries a certain conserved flavor just as in classical DTU. For the time being we continue to treat flavor as an index; later we shall find its origin and interpretation in the quantum surface. Also as in classical DTU, the boundary of Σ_C (the belt) is carved into pieces corresponding to ingoing or outgoing elementary particles. Consistency considerations including the quantum surface eventually will lead us to admit only three kinds of elementary hadrons: mesons, baryons, (antibaryons) and baryoniums. Anticipating the results of Sec. V, the forms of the corresponding belt pieces are shown in Fig. 9, where the arrows are HR orientations transferred to to the boundary. The entire belt is made up from such pieces whose

---

* It will be shown in Sec. VI that the nontrivial belt vertices always occur in "mated" pairs of opposite HR orientation. The two vertices of Fig. 8 are mated.

** After introduction of the quantum surface the representation of electric charge will lead to a "core charge arc", similar in many ways to an HR arc but parallel to a junction line rather than to the belt. Core-charge orientation coincides with HR orientation.

general structure was recognized in Ref. 11. Just as in classical DTU, points along the belt that separate particle pieces are each enclosed by an HR arc; the collection of HR arcs thereby delineates the particle structure of the belt (see Fig. 10).

Again as in classical DTU the surface Σ_C houses a connected open Landau graph (Appendix A); the ends of the graph lie on the belt and correspond to the particles, as indicated by the dotted arcs in Fig. 9. Note how the position of the baryon Landau arc breaks the triangular symmetry of the baryonic piece of belt. It is possible for a baryon Landau arc to cross a junction line, passing from one sheet to another.* Points of such crossing are called glitches and will be found to constitute a measure of entropy (Appendix B).

As in classical DTU the surface Σ_C is divided into ortho and para patches with intervening transition arcs which, if they end on the belt, in strong-interaction topologies, do so at points separating one elementary-particle piece from the next. Since such a point is always enclosed by an HR arc, there must be a crossing of transition arc with HR arc. Transition arcs also may end on junction lines. Attaching classical-patch orientation to patch boundaries gives an orientation to junction-line segments that lie between the end points of transition arcs. The three adjacent patches along such a junction-line segment induce the same parity orientation of the

---

* The reason why meson and baryonium arcs do not "glitch" in strong-interaction topologies will be explained in what follows.

segment, which means that the three patches are either all ortho or all para. All the foregoing rules follow by induction from zero entropy, where as in classical DTU the entire Σ_C is ortho or para--with no transition arcs. The relation of ortho-para orientation of Σ_C to spin dependence and parity inversion is the same as described in Sec. III and Appendix D.

The notion of Landau (multiplugged) connected sum is easily extended to feathered classical surfaces (Appendix B), and will be expressed by the notation

$$\Sigma_C = \Sigma_C^1 \# \Sigma_C^2$$

Corresponding elementary-particle pieces of belt are identified as in classical DTU, a coherent HR orientation of the new surface being ensured if the HR orientations are opposite for a pair of matched belt segments. The connected sum of surfaces is accompanied by similar connected sums of HR arcs and junction lines; HR flavor matching is to be respected. As in classical DTU, when an ortho patch is glued to a para patch, the corresponding piece of belt becomes a transition arc. Otherwise we erase it from the connected sum. Also to be erased from a connected sum is a closed HR loop with disk interior lying within a single classical patch, as is a closed junction line when it is the intersection of an unpatched sphere with a plane.

Figure 9 shows that in baryonium and meson plugs the Landau arcs always can be directly joined to build a new connected Landau

graph on the new classical surface Σ_C. In baryon plugs, however, the two Landau arcs to be connected may reside on sheets that are not united by the connected sum. This mismatch is corrected by an additional glitch and we shall regard as inequivalent the three situations depicted in Fig. 11.* A plug which simultaneously involves a glitch and an O-P transition generates something like Fig. 11C.

What are the special characteristics of zero-entropy classical surfaces from which all strong-interaction Σ_C are to be built by successive connected sums? A zero-entropy classical surface obeys the following requirements:

1°) Each sheet is topologically a disk and consists of a single patch.

2°) There are no glitches, the Landau graph sitting on a single "main sheet" which sees all the particles.

3°) The Landau graph is a tree with a single vertex.

Such demands were also present in classical DTU. The difference is that, there, requirement (2°) is satisfied for all Σ_C--not only zero entropy. The zero-entropy absence of glitches ensures that no Σ_C, achieved through connected sums starting from zero entropy, will ever have junction lines crossed either by meson or baryonium arcs. Appendix B establishes that, in any connected sum leading to a zero-entropy Σ_C, no glitches can appear in constituent classical surfaces; once present, glitches cannot disappear.

The foregoing properties of zero-entropy classical surfaces constrains the zero-entropy belt graph to be extremely simple--a single-stand "necklace of beads", as illustrated by the 2-bead example of Fig. 10. Necklace graphs were introduced in Ref. 11 but

* The trivial Landau vertices discussed in Appendix A clarify this inequivalence.

without an interpretation as the boundary of a multisheeted classical surface; there consequently were no attached Landau arcs. With attachment of Landau and HR arcs to a single-strand necklace graph as in Fig. 10 (HR flavor indices not shown), the zero-entropy topology τ is almost completely specified--all the action residing in the main sheet. The only loose feature is a possible ordering of the two inert sheets belonging to each bead--whose boundaries define the bead within the belt graph.

Giving an order to these inert sheets amounts to ordering the vertices of the belt graph, which in turn amounts to <u>thickening</u> the belt (Appendix B). We shall follow a proposal of Ref. 11 by adding to the structure of Σ_C an <u>ordering of the belt graph</u>.* In more precise terms we postulate that the belt comes with a 2-dimensional thickening which will be an orientable and oriented (also patchwise oriented) surface denoted by $th(\partial\Sigma_C)$. At zero entropy $th(\partial\Sigma_C)$ is planar and the three sheets at each bead are cyclically ordered. Thus a belt graph such as that of Fig. 11 is not zero entropy.

---

* Combining this order with the fact that the Landau graph always gives a special status to one of the 3 sheets can be thought of as attaching one of 3 different and distinguishable <u>topological colors</u> to each sheet at zero entropy (Sec. VIII). The possibility of glitching in connected sums means that beyond zero entropy topological color is not attachable to sheets, but Sec. VIII shows how "color" is attached to the quark lines that embellish a thickened Landau graph.

In giving a precise definition of a feathered topological object τ, we have introduced several arbitrary features: 3 feathers, flavored HR arcs and the special elementary-particle belt pieces of Fig. 9. In our introduction the expectation has been expressed that the interplay with zero entropy of S-matrix unitarity and causality will explain the need for such special features. In Refs. 8, 11, 12 partial explanations have been proposed in terms of ordered (thickened) belt graphs together with the notion of an <u>ordered S matrix</u> whose connected parts are the zero-entropy components of a topological expansion. In this earlier work the belt graph was not recognized as the boundary of a classical surface where Landau and HR arcs reside. We may now, therefore, expect to go further in grasping the consistency implications of zero entropy. It may be that the topological object described in the present section is adequate for such analysis but in the following section we show how the thickened belt is extendable to a <u>closed</u> triangulated surface. Consistency requirements are then much easier to control, especially because at zero entropy the closed surface will be a sphere.

V. QUANTUM SURFACES; GENERAL REQUIREMENTS FOR QUANTUM SPHERES

The previous section introduced the thickening of the belt graph, th $(\partial\Sigma_C)$, a 2-dimensional orientable surface with boundary. Capping off the boundary components with disks then yields a 2-dimensional orientable closed surface--to be called the quantum surface Σ_Q. Note that Σ_Q and Σ_C meet along the belt

$$\partial\Sigma_C = \Sigma_Q \cap \Sigma_C \tag{5.1}$$

At zero entropy each Σ_Q is a sphere, and all higher-entropy strong-interaction Σ_Q will be built from these spheres by connected sums.

Like a Σ_C each Σ_Q will carry additional structures, but before describing these in full we present in this section a collection of natural requirements for zero-entropy quantum spheres. Just as for Σ_C the full characterization of Σ_Q has a circular aspect that depends on zero entropy.

We postulate that any Σ_Q is covered by particle areas which cut the belt into the particle pieces described in the previous section. Anticipating bootstrap results from Sec. VI, we show in Fig. 13 the form of the four distinct particle areas that correspond to the four belt pieces of Fig. 9. Any strong-interaction Σ_Q is completely covered by combinations of these four possibilities. Together with its

division into particle areas, Σ_Q naturally houses the belt; our thickened belt th$(\partial\Sigma_C)$ is, among the various abstractly possible thickenings of $\partial\Sigma_C$, that one uniquely specified as the thickening of $\partial\Sigma_C$ inside Σ_Q (see Appendix B).

Each index τ appearing in the topological expansion corresponds to a surface pair $\Sigma = (\Sigma_Q, \Sigma_C)$ with various attachments, any Landau connected sum of classical surfaces being accompanied by a connected sum of the corresponding quantum surfaces

$$(\Sigma_Q', \Sigma_C') \# (\Sigma_Q'', \Sigma_C'') = (\Sigma_Q' \# \Sigma_Q'' \quad \Sigma_C' \# \Sigma_C'') \tag{5.2}$$

Here $\Sigma_Q' \# \Sigma_Q''$ means "connected sum of closed surfaces "(Appendix B, Subsection 1), there being identification (and erasure) of those areas on Σ_Q' and Σ_Q'' that correspond to the particle pieces of belt identified in $\Sigma_C' \# \Sigma_C''$ --the simultaneous classical-surface "connected sum along the boundary." Complete rules for Landau connected sums of surface pairs are described in Appendix B, attention being given to surface attachments. At zero entropy particle areas are disks and, in connected sums that maintain zero entropy, collections of identified particle areas are also disks; thus zero-entropy connected sums invariably are single plugs.

Because every zero-entropy Σ_Q is an oriented sphere and because, as explained in Appendix B, any Landau connected sum $\Sigma_Q' \# \Sigma_Q''$ of oriented surfaces inherits an orientation from the constituent Σ_Q's, it follows that every strong-interaction component of the topological expansion corresponds to an orientable and oriented Σ_Q. Zero-entropy quantum spheres are furthermore patchwise oriented (Appendix C), a property transmitted via Landau connected sums to all strong-interaction Σ_Q. Because particle-area boundaries lie along patch boundaries, it is possible to characterize most particle areas as clockwise or anticlockwise,* a distinction that we shall connect to the physical distinction between ingoing and outgoing particles or (by crossing, as explained in Appendix D) between particles and antiparticles.

We come now to special zero-entropy quantum-sphere properties not generally shared by higher entropy Σ_Q. In Ref. 3 there was introduced the concept of an ordered Hilbert space. The vectors of this space are labelled not only by elementary-particle momentum and spin but by channel disks which are particle-disk combinations with an attached belt segment and with unique quantum-patch orientations. The belt carries an ortho or para orientation as described above in Secs. III and IV. A connected part of the ordered S matrix is a

* The exceptions correspond to self-conjugate particles like ρ_0-- all of whose quantum numbers are zero.

zero-entropy amplitude corresponding to a surface pair where the quantum sphere is covered by an ingoing channel disk together with an outgoing channel disk. The two disks are joined along their perimeters.

Ordered S-matrix elements are nonvanishing only between channel disks whose perimeters match in an appropriate way. Not only must the number of edges along the perimeters be the same but the quantum-patch orientations must reverse from one channel disk to the next across each perimeter segment. Further attachments to Σ_Q also must match, and belt segments must connect smoothly to form a closed belt graph that is entirely ortho or entirely para. Two ordered channels with the property that the ingoing perimeter of one matches the outgoing perimeter of the other will be said to communicate. The ordered Hilbert space splits into sectors, ordered channels within one sector communicating with each other but not with ordered channels in any other sector. Each sector has a characteristic perimeter.*

It is made plausible in Refs. 8, 11 and 12 that unitarity and analyticity of a cluster-decomposable physical S matrix implies unitarity and analyticity of a cluster-decomposable ordered S matrix. This reasoning preceded the splitting of each ordered sector into ortho and para subsectors, and it has been shown by Stapp that ortho-para splitting conflicts with ordered unitarity.[4] Nevertheless it continues to be true that inversion of Stapp's separate ortho and

* This statement will later become recognizable as a generalized OZI rule.

para S matrices is related in the usual way to analytic continuation in momentum along the "path of Hermitian analyticity"[1]

$$S^{-1} = S_{HA} \quad . \tag{5.3}$$

The ordered S-matrix relation

$$S_{HA}\, S = I \tag{5.4}$$

then leads to the usual discontinuity formulas for ordered connected parts, which provide the basis for calculating masses and amplitudes. Because of the need to give meaning to ordered S-matrix multiplication, the following condition on our topological index and Landau connected sum is natural:

(1) If (τ', κ') and (τ'', κ'') designate zero-entropy components of the topological expansion, then any single-plug connected sum that preserves zero entropy,

$$(\tau', \kappa') \underset{D}{\#} (\tau'', \kappa'') = (\tau, \kappa), \tag{5.5}$$

should be uniquely defined.

Here D denotes the disk that is plugged. In generating higher components of the topological expansion the presence of indistinguishable quantum-surface subareas (such as when there are identical particles) may require several different connected sums of two surface pairs for a given set of intermediate particles. But at

zero entropy it is always possible to divide each quantum sphere into two hemispheres, one of these being the disk D to be plugged. Furthermore by appropriately choosing the signs of particle energies (Appendix D) all particles in one hemisphere can be ingoing while all those in the complement are outgoing. We represent this possibility schematically as

$$\begin{aligned} (\tau', \kappa') &\leftrightarrow (D'_{in}, D_{out}) \\ &\qquad\qquad (5.6) \\ (\tau'', \kappa'') &\leftrightarrow (D_{in}, D''_{out}) \end{aligned}$$

The connected sum Eq. (5.5) then becomes representable as

$$(D'_{in}, D_{out}) \otimes (D_{in}, D'_{out}) = (D'_{in}, D'_{out}) \quad . \tag{5.7}$$

Remembering that the amplitude corresponding to (D'_{in}, D'_{out}) is built from a sum over all intermediate channels, one sees here how zero-entropy connected sums relate to products of matrices. Uniqueness of zero-entropy connected sums is evidently essential to ordered S-matrix multiplication.

The reader may wonder how uniqueness could fail in a single-plug connected sum. The danger lies in a rotational symmetry of the plugged disc that allows the residual (non-plugged) areas of the two quantum spheres to be joined in more than one way. Channel disks with any such symmetry are disallowed by the demand for an ordered S-matrix.[11]

Two additional properties of Landau connected sums ensure "completeness" for the ordered Hilbert space:

(2) In any Landau connected sum, $\Sigma = \Sigma' \# \Sigma''$, both Σ' and Σ'' must be zero entropy if Σ is zero entropy. This rule is a special case of the general entropy property.

(3) Any single-plug connected sum of zero-entropy surface pairs has itself zero entropy if the identified channel disks correspond to "in" and "out" versions of the same vector in the ordered Hilbert space.

Cluster decomposition of the ordered S matrix[8] relates to the notion of quantum-sphere fission. Suppose that a zero entropy sphere is divided into ingoing and outgoing hemispheres, as described above. Suppose further that some ingoing subchannel is adjacent to an outgoing subchannel with the perimeters completely matching. This means that the entire perimeters of these subchannel discs match, not only those portions which necessarily match already on Σ_Q. Under such conditions it is possible to fold onto each other the remaining portions of the matching perimeters and thereby to split the zero-entropy sphere (together with the corresponding Σ_C) into two zero-entropy spheres (each with its Σ_C). When fission is thus possible the ordered S-matrix element contains two terms--one corresponding to a single connected part and the other to a product of two connected parts. If further fission is possible, there will be further products.

The fission process is easily confused with the process of contraction--to be discussed next. The difference is that, under contraction, portions of particle discs disappear while under fission entire particle disks become disconnected from the rest.

Fission describes the physical indistinguishability from forward scattering of no scattering and more generally provides a sense in which an ingoing-outgoing channel pair can be smoothly removed from (τ,κ) without disturbing the remaining particle areas. Contraction instead describes the connection of the single-particle concept to that of the multiparticle bound state and will distinguish strong interactions from electromagnetic and weak interactions. Contraction, a notion introduced by Harari and Rosner,[2] is the topological key to the bootstrap and to quark confinement.

The single-particle disk belonging to a multiparticle channel bound state is achieved by eliminating within the channel disk certain internal areas that do not touch the disk boundary. We require that such contraction of any channel disk belonging to a given sector of the ordered Hilbert space should lead to the same particle disk; every channel disk is uniquely contractible to a particle disk determined completely by the sector perimeter.

Section VI will give a complete and precise definition of what we mean by contraction, including surface attachments, but let us here present a preliminary picture. If on a quantum sphere we see two belt-intersected oppositely-oriented adjacent patches with matching perimeters, the portions [a, b, c] of which are already joined together on Σ_Q as in Fig. 14(a), then we can remove this "mated" pair of patches from Σ_Q, without disturbing the relationship of residual patches, in such a way that the only remnant on the new Σ_Q from these two patches is the segment [a, α=α'; c] shown in Fig. 14(b). This process is like a degenerate connected sum.

An example of the foregoing is shown by the 2-meson channel disk of Fig. 15 contracting to the single-meson disk of Fig. 16, four triangular patches here being reduced to two. The HR graph equivalent of this example is shown in Fig. 17. It may happen, as in a 3-meson disk, that the order of mated-patch removal is not well defined. A general requirement on the patch pattern is that the resulting single-particle disk be nonetheless unique.

The foregoing implies that any zero-entropy quantum sphere is completely contractible--that successive patch-antipatch erasures eventually leave the sphere in the form of a propagator--covered by a single particle disk and the corresponding anti-particle disk. That is, if we consider any particle disk, the complement is a channel disk which contracts uniquely to another particle disk. Now a single-particle to single-particle connected part corresponds physically to nothing happening and so can be nonvanishing only if these two disks correspond to "in" and "out" versions of the same single-particle channel in the ordered Hilbert space or, by crossing, to particle and antiparticle. Because each quantum patch within an "in" particle disc must correspond to an antipatch within the "out" particle disc, we conclude that every patch on a zero-entropy quantum sphere is mated to an antipatch. This topological rule of complete contractibility parallels the familiar algebraic representation of invariance properties through saturation of adjacent tensor or spinor indices; and extends in a natural way the analogy between matrix multiplication and connected-sums.

The existence of two separate indices (τ,κ) attached to components of the topological expansion implies a further requirement on zero-entropy quantum spheres: The pattern of patches on the quantum sphere should uniquely delineate the location of particle areas. The topological index τ then prescribes the location of particle areas while the order index κ assigns momentum and spin values to each area; once the topology is specified, there must be no ambiguity about where one particle area ends and another begins. Section VI will show how to meet this as well as all previously stated requirements.

Some general remarks are now in order about the role of the quantum surface. Our theory represents hadrons as bounded quantum areas (disks, at zero entropy) while reaction amplitudes are represented by closed orientable surfaces covered by particle areas whose boundaries are glued together. This idea, first expressed in Ref. [13], offers a natural description of discrete internal (not directly-observable) quantum numbers through topological attachments along a particle-area perimeter, attachments whose orientations must be matched by those belonging to adjoining particle areas. Conservation of such internal quantum numbers (e.g., flavor) is automatic for closed orientable surfaces. Also natural is associating the "particle-antiparticle" distinction with the two orientations (clockwise or anticlockwise) possible for any quantum patch. A final motivation for Σ_Q is that the bootstrap becomes more tractable than previously thought when formulated as a system of internally-consistent contractions on a spherical surface.

The quantum surface cannot stand alone as basis for the topological expansion. The direct observables--energy-momentum and spin (also electric charge, as will be seen later)--live on the classical surface. A good notion of entropy, furthermore, requires Σ_C; it turns out that the genus of Σ_Q can decrease in certain Landau connected sums. At the same time, as we have already observed, certain features of Σ_C that appear arbitrary in the absence of Σ_Q will become determined in a consistent surface-pair zero-entropy bootstrap.

We close these general remarks with an observation whose significance is obscure but which nevertheless may help the reader to follow the developments of Secs. VI and VII. At zero entropy it turns out that the complete topology of Σ_C may be inferred from Σ_Q and the attachments thereto while the converse is almost but not quite true. (The exception relates to flavor.) Such redundancy, which does not persist in higher orders of the topological expansion, means that the bootstrap problem can be focussed on the quantum surface.

VI. SPHERICAL BOOTSTRAP: LUNAR INSERTION, QUARK CONFINEMENT, BARYON NUMBER AND TRIALITY

This section describes a patch pattern for zero-entropy quantum spheres that is consistent with the requirements of Sec. V as well as with the zero-entropy classical surface of Sec. IV. We shall not establish uniqueness of the pattern but are aware of no satisfactory alternative; many other forms have been considered,* but all have proved deficient. Fulfillment of the bootstrap program requires a uniqueness demonstration, but at the same time there must also be established the existence of an analytic ordered S matrix acting in a Hilbert space of channel disks. The latter question, which involves the Riemann complex-momentum surface corresponding to planar Landau discontinuity formulas, will not be addressed in the present paper.

The pattern to be described--the sole survivor of an extended search--makes successful contact with a variety of established experimental facts and is not known to conflict with any. It will take further work to confirm that this pattern in fact constitutes a complete and correct basis for strong interactions, but optimism is warranted.

Forgetting for the time being about the classical surface, let us consider a triangulation pattern for quantum spheres. That is, our decomposition of Σ_Q into patches is to be the kind of triangulation familiar in the topology of surfaces (or manifolds).

---

* An example of an earlier proposal may be found in Ref. 13.

This fact will be connected below with triality (3 "colors"). Our triangulation, to be called the lunar insertion pattern, was introduced in a dual form in Ref. 11.

Let the quantum sphere be divided into two triangular patches of opposite orientation as in Fig. 18(a). Next split any of the three edges into a "lune" as in Fig. 18(b) and then divide this lune itself into two oppositely-oriented patches as in Fig. 18(c). Such a process can be continued indefinitely and the following features are notable:

1) Triangles occur in "mated" pairs of opposite orientation. A pair of mates is uniquely identifiable by the fact that the corresponding triangles have all three vertices in common (though the two might have no edges in common).

2) Each creation process of a mated triangle pair is the inverse of a contraction, as described in Sec. V. Complete contractibility of the quantum sphere is thus assured.

3) There occur trivial vertices--with only two incident edges--each trivial vertex being shared by an immediately-adjacent pair of mated patches in position to be contracted.

4) Each patch is adjacent to patches of opposite orientation, so our process naturally creates a patchwise-oriented sphere (Appendix C).

5) All trivial vertices lie on the perimeters of particle disks because any particle disk, being maximally contracted, cannot include both members of a mated pair that share a trivial vertex.

The list can be continued; for example it is easy to show that both members of a mated patch pair, whether or not they share a trivial vertex, never occur within the same particle disk. But the above features suffice for the immediate needs.

We proceed next to specify the defining characteristics of a zero-entropy topological index $\tau = (\Sigma_Q, \Sigma_C)$ and to show how these characteristics accommodate the general requirements of Sec. V. The reader should realize that our prescription for zero entropy is not achieved by freezing entropy indices to zero but rather is a direct postulate. Any nonzero-entropy strong-interaction τ is to be achieved from zero entropy by repeated connected sums. It must of course turn out that consistent entropy indices all vanish at our directly-defined entropy zero (and only at entropy zero), but the bootstrap's nonlinearity obliges us to start by guessing the structure of the ordered Hilbert space and only later to verify the consistency of this structure.

We have in Sec. V specified the characteristics of a zero-entropy classical surface Σ_C. A zero-entropy Σ_Q will be a topological sphere, triangulated according to a lunar insertion pattern (hence patchwise oriented), housing the belt $\partial\Sigma_C$, and further such that

A) Σ_Q houses the planar thickened belt, as defined in Sec. V.

B) There are two kinds of triangles: core triangles with no trivial vertex that meet the belt as in Fig. 19(a) at the end of a junction line, and peripheral triangles with (exactly) one trivial vertex that meet the belt as in Fig. 19(b). A peripheral triangle thus intersects a single sheet of Σ_C while a core triangle intersects 3 sheets.

C) The belt's particle pieces are delineated by the trivial vertices of peripheral triangles, as in the example of Fig. 20 which corresponds to Fig. 10. The belt crosses particle boundaries always at a trivial vertex. At the same time the trivial vertices provide unique delineation of the particle discs on Σ_Q. Figure 21 provides an example corresponding to Figs. 10 and 20. The heavy lines are particle boundaries and the dotted lines are the belt. Notice how the heavy boundary lines always separate mated pairs of peripheral triangles and how all vertices (trivial and nontrivial) appear on these boundaries. As required in Sec. V the delineated single-particle disks in Fig. 21 admit no internal contractions. Note also that all multiparticle channel disks in Fig. 21 do admit contraction--to one of the forms exhibited in Fig. 13. Recall the requirement of Sec. V that all sectors of the ordered Hilbert space contain single-particle channels; any multiparticle channel disk must contract to a single-particle disk, and the contractions must not remove any of the peripheral triangles building the channel-disk perimeter.

We are now in position to enumerate the possible elementary hadron disks on Σ_Q. A single triangle is excluded because a 2-particle channel disk with such a constituent would not admit a perimeter-preserving contraction. Anticipating the association (immediately below) of "quark" with peripheral triangle, we have here an explanation of quark confinement. Loosely speaking our explanation amounts to saying that a quark-particle would be incapable of submerging its identity within a bound state; such identity loss, as represented by contraction, constitutes the distinguishing feature

of strong interactions.

In a separate paper on electromagnetism[14] it is shown that single-triangle disks can be associated with charged leptons and introduced together with photons at a complexity level above that of zero entropy. Leptons and photons, once introduced, never lose topological identity--in contrast to hadrons which do so readily in zero-entropy contractions.

The hadron disks of Fig. 13, built from a total of 2, 4 or 6 triangles and containing, respectively, 2, 3 or 4 peripheral triangles, are individually uncontractible and, if combined into multihadron channel disks, the larger areas are uniquely contractible back to one of these four basic forms. A reason for not including elementary-hadron disks with more than 2 core triangles will emerge in Sec. VIII in connection with thickened Landau graphs and topological color. Inclusion of the disk form labeled "baryonium" in Fig. 13 reflects the original Rosner consideration:[2] Once core triangles are admitted, there is no way to exclude from the ordered Hilbert space channel disks with two unmated core triangles. This fact will become clearer in Sec. VIII when we consider thickened Landau graphs.

For each particle disk there is an additively-conserved quantity: the number of anticlockwise core triangles minus the clockwise number. For "out" disks (positive energy, see Appendix D) we identify this quantity with baryon number B; for "in" disks (negative energy) the identification is with -B. Baryon number is conserved for all terms of the topological expansion-- B summing to zero over any Σ_Q. Also conserved is the number of clockwise minus anticlockwise

peripheral triangles, but this latter number invariably is equal to 3B, so there is a single conservation law.* Figure 22 exhibits the foregoing considerations for baryon and antibaryon disks.

Comparison of Fig. 13 with orthodox quark models suggests the term "topological quark" as a synonym for peripheral triangle. The factor 3 between baryon number and quark number has been described as "triality" and we also shall employ this term. We have achieved triality and the related 3-feathered structure of Σ_C by triangulating the quantum surface. Was the choice of triangle as quantum building unit unavoidable?

Suppose that Σ_Q had been divided into squares rather than triangles. The lunar insertion pattern and the notion of trivial vertices would still make sense. However a "core square" would be belted as in Fig. 23(a), which would require an adjacent peripheral square to be belted as in Fig. 23(b). Junction lines then would end on peripheral patches as well as on core patches, and on Σ_C there would be a 3-feathered structure simultaneously with a 4-feathered structure. Such a pattern invites a host of unwanted complications and difficulties absent for triangulation. The triangular patch is the natural a priori choice and its use meshes smoothly with bootstrap requirements.

* Extension to electromagnetism[14] relaxes the factor -3 relation and there appears a new additively-conserved quantity, physically identified with lepton number.

VII. FLAVOR AND ELECTRIC CHARGE

The notion of a topological Hilbert space of channel disks, whose (unbalanced) internal quantum numbers reside along their perimeters, suggests orienting the edges of channel-disk perimeters. This we propose to do. These orientations, which remain unaffected by perimeter-preserving contractions that carry multiparticle disks into single-particle disks, are to be matched when channel disks are fitted together to cover Σ_Q. Since mated peripheral-triangle (quark) pairs are always placed against each other so as to identify edges incident on the belt-intersected trivial vertex, the orientations of these two edges combine to define a 4-valued quark attribute which we call edge flavor.

Figure 24 shows the four edge flavors and the corresponding antiflavors with which each must be matched. Notice that the third edge of a quark triangle--the belt-intersected edge which never lies on a particle-disk perimeter--has not been oriented.* Core triangles, whose edges may lie along such nonoriented peripheral-triangle edges, correspondingly do not carry edge flavor. Defining q_f to be the number of clockwise quarks with edge flavor f minus the anticlockwise number, it follows that q_f is conserved.

In the separate papers on electromagnetism[14] it is proposed that electric charge be carried by oriented arcs on Σ_C, the end of

* In an earlier version of our theory,[5] before introduction of charge arcs, it was proposed to associate orientation of the belt-intersected edge with charge doubling of quarks.

(exactly) one charge arc being perpendicularly attached to each triangle on the quantum surface. Each charge arc, like an HR arc, lies in Σ_C with its ends on the boundary, but HR arcs only couple mated peripheral triangles (quarks). Every triangular patch on Σ_Q has an attached charge arc.*

A peripheral triangle (quark) may be described as "charged" if HR orientation agrees with charge orientation and "neutral" if otherwise.[14] Defining q_c as the number of clockwise charged quarks minus the anticlockwise number, with a corresponding definition of q_o for neutral quarks, it follows that q_c and q_o are separately conserved. For each value f of quark edge flavor, the quark may be either charged or neutral, and the ordinarily-defined quark flavor combines the 2-valued charged-neutral option with the 4-valued f. Hence our theory has a total of 8 conserved quark flavors--4 charge doublets.

Reference 14 shows how the combination of charges attached to peripheral-triangles (quarks) and to core triangles explains the experimentally-observed hadron electric charges. Core triangles turn out always to be charged (never neutral) for a

* For electromagnetic interactions[14] certain "active" charge arcs will connect a triangle on one Σ_Q component with a triangle on a different component. The mate of the first triangle is simultaneously charge connected to the mate of the second. Readers unfamiliar with the contents of Ref. 14 are urged to read at least the shorter of the two electromagnetic papers before proceeding further in the present paper.

reason discussed below in Sec. VIII. Orthodox quark models--with no counterpart of core triangles--achieve the same total hadron charges as topological theory by assigning fractional charge to quarks.

Our topological representation of spin, flavor and electric charge accords with the principle enunciated in Sec. V that (unbalanced) channel-disk quantum numbers all reside on the disk perimeter. By specifying the peripheral-triangle (quark) sequence that builds a channel-disk perimeter, the ordered Hilbert-space sector is completely determined. There is no need to say anything about interior triangles, even core triangles whose mates lie in other channel disks. Core triangles carry neither spin nor edge flavor and, although electrically charged, their charge always may be inferred from quark orientations. The feature that core triangles remain "hidden" within strong interactions* is shown explicitly in the next section by the thickened Landau graph embellished with quark lines, which is shown in Appendix B to convey the entire content of Σ_Q as well as that of Σ_C.

* Core triangles are physically revealed by electromagnetism.[14]

VIII. THICKENED LANDAU GRAPHS AND TOPOLOGICAL COLOR

A feature of classical DTU is a connection between the Riemann surface for the complex-momentum variables of a topological connected part and a thickening, th(L), of the associated Landau graph L. The connection, discussed at length in Ref. 3, is not completely understood, but the dependence of momentum singularities on the cyclic order of Landau arcs in th(L) is central to classical-DTU dynamics.*

We shall not here consider the Riemann surface but, in the expectation that a Landau graph thickening will prove usefully relevant to the structure of complex- momentum singularities, we describe in this section a natural definition of th(L) that goes with any topology $\tau = (\Sigma_Q, \Sigma_C)$.

The reader may be puzzled to find in Ref. 3 no use of the term "thickened Landau graph." The reason is that in classical DTU there is essentially no difference between th(L) and the single-sheeted Σ_C. The thickening can be housed in Σ_C and it is natural to locate HR arcs along the boundary of th(L) with HR orientation agreeing with that of th(L). Adding caps to the ends of HR arcs completes the boundary of th(L). At zero entropy where the Landau-graph is a tree, the only difference between Σ_C and th(L) is a collection of disks along the boundary of Σ_C. These disks remain uninteresting in connected sums because of the contraction rule that always eliminates closed HR loops. Higher components

---

* For example, the order dependence of singularities has led to the inference that Regge branch points are absent from planar connected parts and that planar Regge poles are "exchange degenerate."[3]

of the topological expansion in classical DTU thus perpetuate the essential equivalence of Σ_C to th(L).

With a multisheeted Σ_C the notion of th(L) must be reexamined. Let us start with zero entropy where L is confined to a single sheet. If there are no junction lines, the situation is as in classical DTU, with th(L) embedded in Σ_C and with HR arcs bounding and orienting th(L). With one or more junction lines the only difference is that a core charge arc, rather than an HR arc, runs parallel to each portion of sheet boundary built from a junction line. We are here implicitly assuming that zero-entropy core charge arcs lie on the main sheet of Σ_C.[14] Thus the boundary of th(L) is now composed of HR arcs and core charge arcs; the orientation of the latter agrees with the HR orientation of the sheet. (Hence core triangles always carry electric charge.)

By examining in more detail the zero-entropy pattern one discovers the boundary of a thickened meson arc to be always two HR arcs, as in classical DTU, but the boundary of a thickened baryon arc is one HR arc and one core-charge arc. The boundary of a thickened baryonium Landau arc is two core charge arcs. Figure 25 shows the thickened Landau graph for the example of Figs. 10, 20 and 21. The reader should notice that the core charge arc is playing the role of an "antidiquark-line", a notion that will continue to be valid as we proceed beyond zero entropy.

When a connected sum is made of two zero-entropy surface pairs, $\Sigma = \Sigma' \# \Sigma''$, we postulate an accompanying connected sum of thickened Landau graphs:

$$\text{th}(L) = \text{th}(L') \# \text{th}(L'') \tag{8.1}$$

where corresponding end caps are joined so as to maintain a single coherent orientation. This rule means that HR and core charge arcs connect smoothly. In repeated connected sums the continuity rule allows a coherently oriented th(L) to be associated with the most general surface pair τ.

If τ contains glitches, so that L does not reside entirely on a single sheet of Σ_C, it is not possible to house th(L) in Σ_C. (At a glitch on Σ_C a core-charge arc crosses a baryon arc.) The content of τ is nevertheless not being expanded; each surface pair Σ as previously defined implies a unique th(L).* Each sheet of Σ_C that carries a piece of L, say L_i, houses a corresponding thickened graph $th(L_i)$ (which need not be connected). If the various $th(L_i)$ are coherently sewn together at baryon end caps associated with glitches one constructs th(L):

$$th(L) = th(L_1) \# th(L_2) \# \ldots .$$

It is possible through embellishments of a thickened Landau graph to convey the full topological "history" of a surface pair. Firstly, by including patch boundaries transverse to the Landau arcs, as explained in Subsection 6 of Appendix B [Fig. 45(a)], the patch structure of Σ_C can be represented. Further, along a baryon or a baryonium Landau arc there may occur a "switch"--corresponding to a plug involving a quark permutation, as discussed in detail in Appendix B. The term "switch" is suggested by the "railroad-like" structure of quark lines on th(L).

* The converse is also true, as shown at the end of Appendix B.

Suppose the HR orientation of th(L) is clockwise, so a thickened baryon arc always appears as in Fig. 25, but we choose to represent a core-charge arc by a quark-line pair running the opposite way. A baryon now appears as in Fig. 26(a). The configuration of Fig. 26(b) does not occur; this would correspond to anticlockwise HR orientation. Figure 27 shows how association is possible between each of the 3 quark lines in Fig. 26(a) and a particular triangle in a baryon disk. As discussed in Sec. IX and Appendix B, a baryon plug corresponds to one of 6 different permutations of the 3 quarks. Designating by p a permutation of the two quarks within the diquark ("diquark twist") and by p_+ a clockwise cyclic permutation, the six different baryon plugs correspond to the elements of a permutation group:

$$1,\ p,\ p_+,\ p_+^2,\ pp_+,\ pp_+^2 \tag{8.2}$$

remembering that $p^2 = p_+^3 = 1$ and that $p_+p = pp_+^2$. Each element except the identity permutation we characterize as a "switch" and represent as in Fig. 28. Glitches are recognizable on th(L) as a quark line crossing a Landau arc. It then becomes possible to attach spin-flavor indices to quark lines on th(L).

Notice that quark lines on th(L) do not correspond in a simple way to HR arcs on Σ_C, which never cross either each other or Landau arcs (Appendix B, Subsection 4). A device is here being invoked to keep track within a bonafide 2-dimensional surface of the structure in a multisheeted (singular) Σ_C. For example, as shown in Appendix B, a connected sum of two zero-entropy Σ's through a baryon plug

corresponding to the permutation p ("diquark twist"), leads to a toroidal Σ_Q while the new Σ_C has genus 1. This content for $\tau = (\Sigma_Q, \Sigma_C)$ is unambiguously implied by the p switch of Fig. 28 on th(L).

Baryonium plugs do not include glitches and are confined to the four possibilities

$$1,\ p,\ \bar{p},\ p\bar{p} \tag{8.3}$$

where $\bar{p}$ means interchange of the two antiquarks within an antidiquark. The Fig. 29 representation of baryonium switches on th(L) is self explanatory.

The coupling between baryonium and mesons provides an interesting example of th(L). The transition

$$\text{baryonium} \rightarrow \text{N mesons} \tag{8.4}$$

is forbidden at zero entropy, but the separate transitions

$$\text{baryonium} \rightarrow \text{baryon} + \text{antibaryon} \tag{8.5}$$

$$\text{baryon} + \text{antibaryon} \rightarrow \text{N mesons} \tag{8.6}$$

are allowed. There are then higher-order topologies for Eq. (8.4) corresponding to connected sums with baryon-antibaryon plugs of the zero-entropy surface pairs for Eqs. (8.5) and (8.6). The thickened 2-vertex Landau-graph connected sum is shown in Fig. 30 for 2

final mesons. The result is a cylinder with the baryonium on one boundary and the two mesons on the other. Without switches the baryonium here must have vacuum quantum numbers because the 4 baryonium quark lines connect to themselves; with switches but only 2 vertices the baryonium quantum numbers must be the same as that of a meson ("nonexotic"). With 3 or more vertices and intervening switches, any baryonium quantum numbers can couple to 2 mesons. With or without switches the cylindrical character of th(L) suggests a structure of the Riemann surface here similar to that for OZI-forbidden meson decays such as $\phi \rightarrow \pi\rho$.[3] It is therefore plausible that the dynamical mechanism inhibiting baryonium coupling to mesons is similar to that responsible for the OZI flavor selection rule, which has been extensively explored in classical DTU.[3]

Embellishment of th(L) with quark lines allows recognition of a 3-fold conserved "topological color". That is, as seen in Fig. 27, each quark line in the neighborhood of a Landau vertex carries a "color number", 1, 2 or 3. The "color" can change in a switch, as seen in Fig. 28, but the total number of quark lines with a given "color" remains constant. Elementary mesons carry only color #1 while elementary baryoniums carry only colors #2 and #3. One way to think about the inhibition against baryonium-meson transitions is in terms of topological color.

IX. ELEMENTARY HADRON QUANTUM NUMBERS

Section III has discussed elementary-meson spins and parity, which remain unaltered by quantum-surface considerations and the associated classical-surface feathering. The meson charge-flavor spectrum implied by Σ_Q at zero entropy coincides with that of orthodox quark-model ground states (orthodox models leave arbitrary the number of different charge doublets.) In the present section we show the same statement to be true for baryons and baryoniums although it is less immediate because of the order index κ in the topological expansion. There is only one possible order for the two triangles in a single-meson disk, but several orders are possible for the triangles in a baryon or a baryonium disk; the present section discusses the interaction between order and spin-charge-flavor. We shall not discuss intrinsic parity and merely recall the result of Stapp[4] that ortho-para superposition uniformly leads to "standard" intrinsic parities for all elementary hadrons.

Let us begin consideration of order with baryonium where there is no glitching complication. Single-baryonium disks in the ordered Hilbert space have a definite cyclic order for the four peripheral triangles--two quarks and two antiquarks. Combining electric charge, edge flavor and spin into a single index for each peripheral triangle, a baryonium disk is shown in Fig. 31. Here the clockwise peripheral triangles (e.g. outgoing quarks) carry indices i, j while the anticlockwise peripheral triangles (outgoing antiquarks) carry indices k, l. Each cyclic ordering is a distinct

channel in the ordered Hilbert space, but within the topological expansion [Eq. (2.1)] one sums over all possible orders κ. Although an elementary baryonium is characterized entirely by a pair of quark indices and a pair of antiquark indices, for each elementary baryonium there are 4 distinct ordered 6-triangle disks. Physical significance is lacking for permutations of the two quarks within the diquark or of the two antiquarks within the antidiquark.

Appendix B describes a connected sum where the two identified particle areas differ by a permutation of two quarks. A glance at Fig. 31 shows this connected sum not to be a simple plug, as discussed already in Sec. VIII. But for the purposes here only two points need be drawn from Appendix B:

a) A Landau connected sum is well-defined (unique) when the identified particle areas differ by a permutation of two quarks.*

b) Entropy increases in such a connected sum.

Taken together these two facts allow consistency between single-baryonium channels of the ordered Hilbert space and single-baryonium channels of the smaller Hilbert space in which the topological expansion is defined. Summation over κ in Eq. (2.1) includes a sum over quark (and antiquark) permutations within particle disks. For each baryonium disk there are four different triangle arrangements.

* When two quarks carrying the same charge-spin-flavor appear within a single-particle disk, plugs are to be made with and without permutation, just as for nonidentical quarks.

Permutation summation produces the same effect on the elementary baryonium spectrum as achieved for ground states of orthodox quark models by assigning 3 colors to quarks, requiring Fermi statistics, and assigning diquarks to antisymmetric color triplets. The net result for orthodox models is to require symmetry under simultaneous interchange of spin-charge-flavor. Such symmetry is an automatic consequence of permutation summation within the topological expansion.

Baryon disks also admit quark permutations, but now there are 6 distinct possibilities. Here we must pay attention to the location on the disk of the baryon Landau-arc's end. For meson and baryonium disks the Landau arcs end in the disk "center", but as shown earlier in Figs. 9 and 27 the position of the baryon Landau arc breaks a triangular symmetry; before assignment of spin-charge-flavor, the three quark positions in a baryon disk are already distinguishable. With regard to the "quark-diquark" terminology of Sec. VIII, the peripheral triangle touched by the baryon Landau arc is "the quark" while the untouched pair of peripheral triangles constitute "the diquark." Permutation summation within the topological expansion means that an elementary baryon corresponds to a superposition

$$1 + p + p_+ + p_+^2 + pp_+ + pp_+^2 \qquad (9.1)$$

which is symmetric under all quark permutations. At the same time the topology of an individual baryon plug depends on the permutation relating the two identified 4-triangle areas; and only the plug corresponding to the identity permutation fails to increase entropy.

Thus we may consistently associate individual 4-triangle disks with single-baryon channels of the ordered Hilbert space while at the same time summing over all six quark permutations in the topological expansion.

For reasons similar to those for baryonium, our elementary baryon spectrum coincides in spin-charge-flavor content with the ground states of orthodox quark models. The orthodox approach assigns all physical particles to color singlets, which for baryons means a 3-quark configuration totally antisymmetric in color. Fermi statistics then imply symmetry in spin-charge-flavor, in agreement with Eq. (9.1). The upshot then is that our elementary hadrons have all the same quantum numbers as the 2, 3 and 4-quark ground states of naive quark models.

X. TOPOLOGICAL SUPERSYMMETRY AT ZERO ENTROPY

The structure of the discontinuity formulas that connect (and hopefully determine) zero-entropy amplitudes does not change when applied to differing numbers of quark lines-- 2, 3, or 4--embellishing a thickened Landau arc. The Stapp rule (Appendix D) allows zero-entropy quark-spin dependence to be represented (like electric charge) by a 2-valued conserved index on each quark line. This dependence factors completely from the momentum dependence, which may consequently be associated at zero-entropy with the unembellished Landau graph. The bootstrap problem is thereby vastly simplified--being reduced to the planar discontinuities of spinless, flavorless connected parts. Elementary mesons, baryons and baryoniums all share a single mass.* Their M functions (Appendix D) differ only by trivial Kronecker delta-function factors in spin and flavor indices. Following Ref. 15 where the concept was first emphasized, we refer to this zero-entropy pattern as "topological supersymmetry", because it places bosons and fermions into a single supermultiplet.

It is evident that topologies with switches (glitches and diquark twists) will break topological supersymmetry. In fact ortho-para transitions already do so--coupling spin dependence to particle momentum. Whether the observed mass differences between mesons and baryons can explained quantitatively by our theory remains unknown

* At this stage of our understanding it is conceivable that the universal zero-entropy elementary hadron mass is zero.

at this point.*

Topological supersymmetry implies flavor symmetry, which is experimentally observed to be badly broken with respect to masses. Appendix D discusses a possible coupling of flavor with spin and "topological color" that can break flavor symmetry when switches occur.

* It is noteworthy that the observed mass splitting between spin 0 and spin 1 mesons is as large as the observed splitting between mesons and baryons.

XI. CONCLUSION: QCD vs. DTU

This paper has described a DTU theory of strong-interaction quantum numbers. Omitted have been the flavor-symmetry breaking and complex-momentum Riemann-surface considerations needed to predict hadron masses, but analytic S-matrix developments during two decades of general S-matrix theory and almost one decade of classical DTU are compatible with the topological structure described here. In the combination of topological entropy with unitarity-analyticity we believe there resides a complete and unique theory at least of strong interactions. Parallel DTU work by Stapp with emphasis on Landau singularities[4] is providing support for such optimism, as is the extension to electromagnetism[14] which is found to fit naturally with the framework described here. Prospects are excellent for a further extension to unified electroweak interactions.

Topological bootstrap theory proposes to explain not only hadron quark structure but quark attributes--spin, color, flavor and electric charge; these are not arbitrary and do not always assume the forms familiar in quantum chromodynamics (QCD). Quarks can be said to carry one of three conserved "colors", but there is no continuous SU_3 color symmetry; topological color permutations are discrete and gluons need not be mentioned. Nevertheless, it turns out that the spin, parity, electric charge and flavor of elementary hadrons in topological theory coincide with those of ground states in orthodox quark models.

The triangular character of Σ_Q patching leads not only to 3 "colors" but uniquely to 8 flavors--4 doublets each containing one charged and one neutral quark. Topological quarks carry integral electric charge, like leptons, in contrast to the fractional charges of orthodox models, but core triangles also carry charge and the total charges of elementary hadrons in topological theory agree with those of their physical counterparts.[14]

Although core triangles possess neither spin nor flavor, they are the unique carriers of baryon number. Elementary hadrons contain either zero, one or two core triangles, the latter case corresponding to baryonium which in DTU plays a more significant role than in orthodox quark models. Although baryonium can decay into mesons, such communication is inhibited, because of core triangles, to a degree at least as great as that of the usual OZI rule.[3] The prediction of a family of baryonium states with properties closely and predictably related to those of mesons and baryons is a distinctive and experimentally testable feature of DTU.

Classical DTU has found that rapid convergence of the topological expansion beyond the planar level is confined to the region of small transverse momentum ($p_\perp$).[3] Planar amplitudes fall exponentially in magnitude with increasing $p_\perp$ and are rapidly overtaken by non-planar corrections, so to describe large $p_\perp$ even approximately it is necessary to sum over components of high complexity. At the same time, model calculations of the cylinder and related toroidal components (Reggeon calculus[8]), have shown how orthodox linear techniques can build on planar components to yield understanding

of phenomena where the planar approximation fails. We therefore expect DTU in principle to describe strong interactions at both large and small $p_\perp$.

At the same time we anticipate that from the summation over high-complexity components there will develop high-$p_\perp$ regularities not immediately apparent at the planar level and even less visible at zero entropy. Our expectation here is motivated by classical physics. Extension of topological theory to electromagnetism[14] has allowed a one-to-one identification of Feynman graphs in quantum electrodynamics with (noncontractible) surface pairs, the number of photon vertices being an entropy index. A large number of photons thus means large complexity, even at low $p_\perp$, and classical physics becomes a limit of extremely high entropy. Now classical physics exhibits collective low-$p_\perp$ regularities such as rigid-body motion of "real objects", that are unanticipated from first quantum principles; it is plausible that there will be analogous high-entropy collective regularities in the high-$p_\perp$ domain of strong interactions. Such regularities may include successful aspects of QCD such as the parton limit associated with asymptotic freedom. The parton idea, which attributes momentum to "current quarks", is hard to understand from the DTU viewpoint, which attaches discrete quantum numbers but not momentum to topological quarks. In a high-entropy limit, however, where continuous space-time begins to acquire meaning, perhaps parton momentum will also achieve approximate significance.

Because the observable space-time continuum is meaningful only in classical physics (the "real world"), we suspect that significance for the local field notion requires a domain of large complexity; the space-time continuum may lack absolute meaning and represent an approximate high-entropy collective regularity. The time notion, for example, might be understandable as an average measure of entropy growth. Support for such conjectures comes from the fact that quantum field theory has achieved useful significance only through perturbative expansions around "classical" limits. In QCD the relevant domain is high $p_\perp$; the existence of individual hadrons has not yet been explained.

Combining the foregoing considerations we are led to suggest that QCD has meaning only as a high-$p_\perp$ approximation and is inapplicable for physics characterized in DTU as "low entropy". The tolerance of QCD for variation in the number of colors and flavors we then find understandable because the bootstrap constraint on hadron quantum numbers arises at zero entropy. The need in QCD to assign fractional charges to quarks we attribute to a high-entropy averaging that obliterates memory of core triangles in somewhat the same sense that baryon number becomes lost in classical physics. Local color gauge invariance--a cornerstone of QCD--we conjecture to have no significance near zero entropy but to emerge, together with the local-field concept, near a "classical" limit. Generally speaking, all physically-useful continous notions we see as high-complexity "collective" approximations to an

underlying discrete structure.*

To the extent that currently-available methods for evaluating predictions of QCD and DTU apply in nonoverlapping domains (high $p_\perp$ and low $p_\perp$, respectively), it is difficult to arrange an experimental confrontation. If the DTU prediction of 8 flavors is successful, the value of topological theory will be established, but QCD would not thereby be shown wrong-- only incomplete. The apparent "glueball" prediction from QCD[15] is interesting but indecisive. There are no glueballs among elementary DTU hadrons, but composite glueballs (analogous to deuterons) cannot be ruled out as consequences of higher entropy. On the other side of the coin, no QCD proof has been given that glueballs must exist. QCD is similarly unsure about baryoniums; metastable baryoniums seem unlikely in a theory with no counterpart of core triangles but, because low $p_\perp$ is involved, field theory has not made a secure statement. Although the core triangles of DTU remain invisible with respect to strong interactions, it is possible that certain spin-sensitive electromagnetic properties of baryons will be affected in an experimentally-testable way, allowing a distinction from QCD. This question is receiving attention but the answer so far remains uncertain.

---

* The energy-momentum continuum is a consistent adjunct of DTU because measurement of energy-momentum is inevitably classical-- involving highly complex systems with many photons.

It may be hoped that extension of DTU to weak interactions will yield certain predictions different from those of field theory. The complexity associated with nonorientable topological objects, so far unutilized in our theory, is crying to be recognized as physically relevant. Because DTU couples electric charge to surface orientation,[14] the C, P topological structure of weak charged and neutral currents may have unorthodox consequences. It also appears that core triangles make the breaking of baryon-number conservation more difficult than in field theory.

Added note:

Implicit in the zero-entropy topology described in this paper but nowhere discussed explicitly is a feature that independently doubles each quark: the relative order of the quark charge and spin (HR) arcs. This order must be preserved in zero-entropy plugs, so that charge and spin arcs do not cross on Σ_C, but generally there may be "quark twists" with a corresponding increase of entropy. The charge-spin order within a quark, like classical-patch orientation and topological color, is a "hidden variable"--always summed over before contact is made with experimentally-measureable amplitudes.

APPENDIX A: LANDAU GRAPHS

The term Landau graph as originally introduced in general S-matrix theory to describe connected-part singularities[1] is a connected open graph with the following additional properties:

a) Every vertex has at least 3 incident arcs (no trivial vertices).

b) No arc connects a vertex to itself.

c) It is possible to find an ordering of the set of vertices, v_1, $v_2 \cdots v_n$, and a system of orientations for the arcs, such that every vertex has both incoming and outgoing arcs, and no arc goes from a vertex of higher index to one with lower index. The ordering and orientations in question are not unique.

In such graphs vertices may be associated with causally-connected "events", each event having both a past and a future. Arcs may be given a particle interpretation; an energy-momentum four vector may be attached to each arc,* with the conservation law that the total flow of energy-momentum into any vertex is zero. Although reference is made in Property (c) to arc orientation, Landau arcs are not oriented. The distinction between ingoing and outgoing particles arises from the sign of the particle energy (see Appendix D) not from Landau arc orientation. Properties

* Although energy-momentum depends on the Lorentz frame of reference, each particle has a unique mass. Thus Landau arcs are labeled by particle masses.

(b) and (c) may be restated in combined form without reference to orientation as:

d) No vertex is allowed where a cut can isolate a closed subgraph (see Fig. 32).

In an ordered Landau graph the arcs incident on each vertex are placed in a definite cyclic sequence. The distinction between ordinary S-matrix theory and topological S matrix theory lies in the distinction between ordinary Landau graphs and ordered Landau graphs. The latter admit a unique thickening--which is housed within Σ_C in classical DTU, where the HR graph lies along the boundary of the thickened Landau graph. Section 8 has described a general relation between th(L) and Σ_C.

Ordinary (non-ordered) Landau graphs describe the nature and location of isolated complex-momentum singularities of physical S-matrix connected parts. The book by Iagolnitzer[1] may be consulted for the detailed set of Landau singularity rules. We here state only the most basic aspects: A single-vertex ordinary Landau graph corresponds to an S-matrix connected part, while any multivertex ordinary Landau graph G corresponds to a singularity of the connected part belonging to the graph resulting from contraction of G to a single vertex (without internal arcs). For example, if cutting a single arc of a 2-vertex Landau graph disconnects the graph, then this arc corresponds to a pole with a factorized residue; the two factors of the residue correspond to the two single-vertex connected-part graphs that result from the cut. The location of the pole is determined by the particle mass attached to the cut arc.

With ordered (thickened) Landau graphs the rules are related to the foregoing but different, being dictated by the topological expansion in conjunction with Landau connected sums based on zero entropy. Although the graphs directly built by connected sum from zero entropy will satisfy conditions (a), (b) and (d) above, contractions may violate these conditions. Both closed loops and trivial vertices must be admitted. What are the contraction rules?

In classical DTU, where there are neither classical patches nor switches (Sec. VIII) two kinds of contraction are allowed:

(1) Two "parallel" internal Landau arcs may be contracted to a single arc. "Parallel" means that the arc pair is incident on the same pair of vertices in immediate sequence at both vertices but in opposite cyclic order so that the arcs are embeddable on a planar surface without crossing.

(2) Any internal arc connecting a pair of different vertices may be shrunk to a point so that the two vertices become one vertex.

Although in classical DTU these rules always lead to a single surviving vertex, certain internal arcs may survive, as in Figs. 3 and 4. The contracted graph with some minimum number of internal loops is not generally unique (i.e., depends on the order in which contractions are performed), but we define as topologically equivalent (belonging to the same τ, κ) any pair of graphs related by a "duality" transformation which slides an external arc along the boundary of the thickening of internal arcs, without crossing another external arc. Figure 33 gives examples of duality-equivalent single-vertex Landau graphs. Fully-contracted ordered Landau graphs are

unique up to a duality transformation. Any such graph may be completely characterized by the genus and boundary structure of the thickening of its internal loops. For example the graph of Fig. 33(a) has genus 0 and two boundary components, with external arcs arranged in the cyclic (clockwise) sequences ABC and FED. The graph of Fig. 33(b) has genus 1 and a single boundary component with external arcs in the cyclic sequence DCBA.

It is easy to verify that any momentum singularity of a zero-entropy connected part corresponds to a multivertex Landau graph that can be contracted to a single vertex tree--without internal loops. Weissmann[8] has shown that Eq. (2.5) implies all the ordinary Landau singularity rules for the ordered S matrix built from zero-entropy connected parts.

Classical patching assigns an ortho or para status to each vertex of an ordered (thickened) Landau graph. Two adjacent vertices may be contracted to a single vertex only if both are ortho or both para. If not, all arcs connecting these vertices must be kept. Contraction now may lead to trivial vertices as shown by the example of Fig. 34(a).

The thickened Landau graph associated with a feathered classical surface has an additional feature that inhibits contractions. Any baryon or baryonium arc may carry a "switch" (Sec. VIII) and switches never disappear (Appendix B). Adjacent Landau vertices connected by arcs with switches may not be contracted to a single vertex, even if both are ortho or both para, and there develops a new source of trivial vertices, as shown by the example of Fig. 34(b).

APPENDIX B: CONNECTED SUMS, PLUGS, THICKENINGS AND ENTROPY

This appendix, being relatively long, is divided into several subsections.

1) Review of usual topological connected sums.

Already in a purely topological sense the notion of "connected sum" is defined in a variety of interrelated contexts. We shall refer to any of these usual notions as a "topological connected sum". The "Landau connected sum" employed in this paper generalizes the topological connected sum in several respects; the additional ingredients will be introduced here one at a time as they become needed.

The usual topological connected sum # is defined in the four different contexts represented in Fig. 35. Although the manifolds of concern in this paper are all of dimension $n \leqslant 2$, most of the statements in this subsection apply to higher dimensions.

In the context I with dimension n = 2 we have two oriented, closed, connected surfaces S_1 and S_2. One considers two disks $D_1 \subset S_1$ and $D_2 \subset S_2$ which one glues together so that their orientations, coming respectively from S_1 and S_2, are mismatched. From the union $S_1 \cup S_2$ so obtained one erases the common interiors of D_1 and D_2, leaving a new closed connected surface $(S_1 - \text{int } D_1) \cup (S_2 - \text{int } D_2)$. On this surface the orientations of $S_1 - \text{int } D_1$ and $S_2 - \text{int } D_2$ fit together into a unique coherent orientation and the resulting oriented surface is by definition $S_1 \# S_2$ in the context I.

The operation is commutative and associative. Moreover one has the following formula for the genus

$$g(S_1 \# S_2) = g(S_1) + g(S_2) \tag{B.1}$$

We adopt here the convention that the genus of a torus with h handles is 2 h. Formula (B.1) implies that the usual 2-sphere S^2 plays the role of a unit for the operation #. This formula, which we later will recognize as an entropy property, excludes the possibility of nontrivial inverses for #.

Still in the context I we make the following remarks:

A) Specifying the gluing map $D_1 \to D_2$ leaves no ambiguity about the defined object $S_1 \# S_2$.

B) The operation # makes sense in an arbitrary dimension n, provided of course that one makes a connected sum of manifolds of the same dimension.

C) In sufficiently high dimensions nontrivial inverses may exist.

We pass now to context III (nonoriented manifolds). This is a straightforward generalization of I except that uniqueness of the resulting object $S_1 \# S_2$ (up to homeomorphism) does not immediately follow, since the gluing map $D_1 \to D_2$ is arbitrary. Nevertheless, either of the following 2 conditions assures uniqueness.

i) One or both of the ingredient surfaces is nonorientable.

(The connected sum is then also nonorientable. The reader is cautioned not to confuse the terms "nonoriented" and nonorientable".)

ii) One of the two surfaces is orientable and admits a homeomorphism which reverses the orientation. This requirement is always met in dimensions n = 1, 2.

For a general closed surface with h handles and ℓ crosscaps we define the genus by $g = 2h + \ell$. Formula (B.1) then continues to hold.

We pass now to context II--the sum of two connected n-dimensional oriented and bounded manifolds, M_1 and M_2. The boundaries ∂M_1 and ∂M_2 are naturally oriented (the orientations being induced by the orientations of M_1 and M_2, respectively) and of dimension n - 1. We shall speak now as if n = 3, but everything works similarly in the general case.

One takes disks $D_1 \subset \partial M_1$ and $D_2 \subset \partial M_2$ and glues them together so that their orientations mismatch. The connected union $M_1 \cup M_2$ then has a coherent orientation coming from M_1 and M_2. Denoting this connected sum by $M_1 \# M_2$ (context II) one has

$$\partial(M_1 \# M_2) = \partial M_1 \# \partial M_2 \quad \text{(context I)}.$$

The extension to context IV is straightforward.

2) Connected sums for surface pairs.

The topological index τ for our theory of strong interactions, as well as for the extension to electromagnetism,[14] consists of a "surface pair" (Σ_Q, Σ_C) with some extra structures. Here Σ_Q is a closed oriented surface, with some mild singularities to be described below, and Σ_C is a 3-feathered surface with boundary

$$\partial\Sigma_C = \Sigma_C \cap \Sigma_Q,$$

which we call the belt. In this section we do not use the entire structure of $\tau = (\Sigma_Q, \Sigma_C)$ but refer only to the features that Σ_Q is oriented and patchwise-oriented, while each sheet of Σ_C is HR-oriented and also patchwise oriented (as explained in Sec. IV). The quantum surface is divided into triangles which are exactly the patches of the patchwise orientation. This means that any edge, adjacent to triangles T', T" receives a common patch-induced edge orientation (not to be confused with edge-flavor orientation) from T' and T".

Already at the level of the quantum surface Σ_Q alone, we shall need multi-plugged connected sums, as opposed to the single-plugged connected sums considered above in Subsection (1). Precisely, we shall perform connected sums $\Sigma_{Q'} \# \Sigma_{Q''}$ where disks $D'_1, \ldots D'_k \subset \Sigma_{Q'}$ are plugged against $D''_1, \ldots D''_k \subset \Sigma_{Q''}$. We will always assume the following:

(1) The gluing of D'_i to D''_i mismatches the orientations (as in Case I of Subsection (1)) so that the global orientations of $\Sigma_{Q'}$ and $\Sigma_{Q''}$ match to a global orientation of $\Sigma_{Q'} \# \Sigma_{Q''}$.

(2) Each triangle $T' \subset D'_i$ is plugged against some triangle $T'' \subset D''_i$ of opposite orientation in such a way that patch-induced edge orientations match. In this way $\Sigma_{Q'} \# \Sigma_{Q''}$ inherits a patch-orientation from $\Sigma_{Q'}$ and $\Sigma_{Q''}$.

It may happen that D'_i and D''_j touch, with D''_i and D''_j touching or not (or the other way around). This possibility has several consequences:

(3) Our quantum "surfaces" may have singularities of the type shown in Fig. 36, although nothing worse.

(4) Relations of the type (B.1) may be violated for quantum

surfaces. Our Σ_Q's will not generate any "entropy indices".

Just as our $\Sigma_{Q'} \# \Sigma_{Q''}$ is a multiplugged generalization of the topological connected sum I, the associated connected sum $\Sigma_{C'} \# \Sigma_{C''}$ will be a multiplugged generalization of II. To achieve consistency between classical and quantum connected sums the following further requirements are imposed on Σ_Q connected sums:

(5) An edge cut by the belt must be identified with another belt-intersected edge and a vertex cut by the belt must be identified with a belt-intersected vertex.*

With the foregoing requirements, when we perform a connected sum for the full surface pair

$$(\Sigma_Q, \Sigma_C) = (\Sigma_{Q'}, \Sigma_{C'}) \# (\Sigma_{Q''}, \Sigma_{C''})$$

one has disk plugs

$$D'_1 \ldots . D'_k \subset \Sigma_{Q'} \quad \text{and} \quad D''_1 \ldots . D''_k \subset \Sigma_{Q''}$$

which carve out 1-dimensional "piece" plugs from the corresponding belts:

$$A'_i = D'_i \cap \partial\Sigma_{C'}, \quad A''_i = D''_i \cap \partial\Sigma_{C''}$$

* With a required matching of edge-flavor orientations (described in Sec. VII), any two particle areas whose triangles can be plugged together by these rules represent in-out versions of the same physical particle.

and when D'_i is plugged against D''_i the piece A'_i is plugged against A''_i, with all HR orientations mismatched. After gluing D'_i to D''_i and erasing int $D'_i - A'_i$ (and hence also int $D''_i - A''_i$) one achieves a new surface pair

$$(\Sigma_{Q'}, \Sigma_{C'}) \# (\Sigma_{Q''}, \Sigma_{C''}) = (\Sigma_{Q'} \# \Sigma_{Q''}, \Sigma_{C'} \# \Sigma_{C''}).$$

One notices that $\Sigma_{C'} \# \Sigma_{C''}$ naturally inherits a patch structure from $\Sigma_{C'}$ and $\Sigma_{C''}$ and if one denotes the number of 0-P patches by $p(\Sigma_C)$ then

$$p(\Sigma_{C'} \# \Sigma_{C''}) \geqslant \max \left(p(\Sigma_{C'}), p(\Sigma_{C''})\right) \tag{B.2}$$

To proceed further we need some additional definitions. Denote by M the Möbius band and by T the punctured torus ($T = S^1 \times S^1$ minus a disk). By definition a feathered Σ_C will be called orientable if it does not house any copy of M and nonorientable otherwise. (Each separate sheet of Σ_C is orientable but M might cross junction lines.) For an orientable Σ_C we define the genus $g(\Sigma_C)$ to be twice the maximum number of disjoined T's which we can embed in Σ_C, with possible crossing of junction lines. For a nonorientable Σ_C consider any family F consisting of disjoined M's and T's embedded in Σ_C:

$$F = \{M_1, \ldots, M_\ell, T_1, \ldots, T_h\}$$

By a straightforward generalization of a similar argument for smooth surfaces one can change F into a similar family

$$F' = \{M_1, M_2 \ldots . M_{2h+\ell}\}$$

Moreover when F is maximal so is F' (and conversely). By definition the maximal $2h + \ell$ is the genus $g(\Sigma_C)$ in the nonorientable case. With these definitions one finds

$$g(\Sigma_{C'} \# \Sigma_{C''}) \geq g(\Sigma_{C'}) + g(\Sigma_{C''}) \qquad (B.3)$$

Remarks: (a) Our notion of classical-surface genus is a straightforward generalization from the smooth case (no junction lines) well known in classical DTU.

(b) The (possible) inequality in Eq. (B. 3) arises from the multiplugged character of the connected sum.

We shall also consider the quantity $b(\Sigma_C) \equiv$ {the number of connected components of $\partial\Sigma_C$}. In the smooth classical-DTU case this is just "the number of boundaries". Now in making our multiplugged connected sum $\Sigma_{C'} \# \Sigma_{C''}$ let us think of the various plugs being made successively, passing from a first connected object $\Sigma(1)$ to successive objects $\Sigma(2), .., \Sigma(n) = \Sigma_{C'} \# \Sigma_{C''}$. After the first step one has

$$g(\Sigma(1)) = g(\Sigma_{C'}) + g(\Sigma_{C''})$$

and

$$b(\Sigma(1)) = b(\Sigma_{C'}) + b(\Sigma_{C''}) - 1.$$

Then, in passing from $\Sigma(j)$ to $\Sigma(j+1)$ one of the following things can happen:

a) The 1-dimensional piece plugs A'_{j+1} and A''_{j+1} are on different components of the belt $\partial(\Sigma(j))$ but do not <u>both</u> exhaust those components. In that case g increases by 2 units and b decreases by one unit.

b) Each of the A'_{j+1} and A''_{j+1} constitutes an entire belt component. Then g increases by 2 units and b decreases by 2 units.

c) A'_{j+1} and A''_{j+1} are on the same belt component but not adjacent. There are two subcases: (c-1) The number of Möbius bands increases. Then g increases by one unit and b stays constant. (c-2) Otherwise g stays constant and b increases by one unit.

d) If A'_{j+1} and A''_{j+1} are adjacent on the same belt component and do not exhaust it, then nothing changes so far as g and b are concerned.

e) A'_{j+1} and A''_{j+1} together exhaust a belt component. Then g stays constant and b decreases by one unit.

We see that, except for Case (e), when b decreases there is an increase in g by at least the same amount. Case (e) can occur exactly when an <u>entire</u> belt component $B' \subset \partial\Sigma_{C'}$ is identified to an entire belt component $B'' \subset \partial\Sigma_{C''}$. Let us assume that there are exactly q such occurrences

$$B'_1, \ldots . B'_q \subset \partial\Sigma_{C'} \text{ and } B''_1, \ldots . B''_q \subset \partial\Sigma_{C''}$$

Now for physical reasons $b(\Sigma_{C'}) > q$ and $b(\Sigma_{C''}) > q$. This is because our classical surfaces house Landau graphs and our # are matched by corresponding Landau connected sums of the graphs. The vertices of a Landau graph represent time-ordered causally-connected events. It is therefore impossible for <u>all</u> the arcs incident on a Landau vertex to pass to a single neighboring vertex. (Energy-conservation also can be

invoked to preclude disappearance of an entire $\partial\Sigma_{C'}$ or $\partial\Sigma_{C''}$ in a connected sum.)

So Case (e) splits into the following subcases:

e.1) $q > 1$. Then the total contribution of the q gluings of B_i' to B_i'' is a decrease of b by 2q and an increase of g by at least 2q-2 (assume that the first step passing to $\Sigma(1)$ is replaced by these q gluings).

e.2) $q = 1$. Then g does not change while the total b has decreased by two units (to $b(\Sigma_{Q'}) + b(\Sigma_{Q''})-2$). Two conclusions may be drawn from this analysis:

α) Defining the quantity $j(\Sigma_C) \equiv b(\Sigma_C) + g(\Sigma_C)$ there is the property

$$j(\Sigma_C) \geq \max\left(j(\Sigma_{C'}), j(\Sigma_{C''})\right) \qquad (B.4)$$

Proof: This is obvious in cases a through d. In Case (e) one has

$$j(\Sigma_{C'} \# \Sigma_{C''}) \geq g' + g'' + b' + b'' - 2$$

Now if $q > 1$, then $b' > q \geq 2$ and $b'' > q \geq 2$, which implies

$$j(\Sigma_{C'} \# \Sigma_{C''}) > \max\left(j(\Sigma_{C'}), j(\Sigma_{C''})\right)$$

If $g = 1$ then $b' \geq 2$ and $b'' \geq 2$, which implies

$$j(\Sigma_{C'} \# \Sigma_{C''}) \geq \max\left(j(\Sigma_{C'}), j(\Sigma_{C''})\right)$$

The fact that a combination of g and b, as well as g, possesses an entropy property, allows control of g and b in the topological expansion.

β) In terms of g and b only two self-reproducing situations are allowed:

β.1) $g = 0$ and $b = 1$, which corresponds to "planar", a characteristic of zero entropy.

β.2) $g = 0$ and $b = 2$, which corresponds to the "cylinder".

(The fact that a cylinder can reproduce itself does not conflict with the fact that the cylinder may be built by connected sum from two planar Σ_C's. On the other hand, the self-reproducibility of the cylinder is important to the topological theory of photons[14] and pomerons.[3])

3) Thickenings

The subject of thickenings is an important and complicated topic in topology. We shall here give only a sketchy intuitive glimpse--the bare minimum for our needs. For more details the reader may consult "A Course in Simple - Homotopy Theory" by M. M. Cohen (Springer, 1970) or either of the following papers: "Simplicial spaces, nuclei and m - groups" by J. H. C. Whitehead (Proc. Lond. Math. Soc. 45, 1939, pp. 243 - 327); "Whitehead Torsion", by J. Milnor (Bull. A. M. S. 72, 1966, pp. 358 - 426).

The general idea is the following. Consider some "space" X, such as a graph or a feathered surface. Choose some dimension $n > \dim X$. Is it possible to "thicken" X into an n-dimensional smooth manifold? Or, in slightly more precise terms, is it possible to find a smooth compact bounded n-dimensional manifold A^n, containing X and collapsing on X in a nice way? The notion of "collapsing" is defined explicitly in the references listed above, but we try now to convey an intuitive feeling by examples.

I. Two-dimensional thickening of a graph. Consider the single-vertex, 2-arc graph of Fig. 37. There are exactly eight distince 2-dimensional ways to thicken this graph, depicted in Fig. 38. The A^2 thickenings are, respectively, (a) a sphere with 3 holes, (b,c) a Möbius band with one hole, (d,f,g) a Klein bottle with one hole, (e) a torus with one hole, and (h) a Klein bottle with two holes. Although

in Figs. 38(b) and 38(c) [and similarly in Figs. 38(f) and 38(g)] the space A^2 is the same, the thickenings are different since in one the Möbius band sits around γ and in the other around γ. In more formal terms a thickening A is endowed with a collapsing map $A \underset{\pi}{\to} X$ which retracts it on X. Two thickenings are equivalent if there is a commutative diagram as in Fig. 39.

Generally speaking 2-dimensional thickenings of a graph Γ are completely specified by

i) some cyclical order of the edges around each vertex

ii) for each closed circuit $C \subset \Gamma$ one has to specify whether, along C, the thickening is orientable or not. The thickened Landau graph th(L) is the particular 2-dimensional thickening of the ordered Landau graph (Appendix A) obtained by demanding global orientability.

II. Whenever X is already embedded in some n-manifold M^n, there is a more or less unique way to thicken X inside M^n; this will be denoted by $N(X; M^n)$ and is called the "regular neighborhood of X in M^n". In classical DTU, $th(L) = N(L; \Sigma_C)$. More generally this statement holds for each separate (smooth) sheet of Σ_C. With glitches, however, the full th(L) described in Sec. VIII cannot be housed in Σ_C.

The following fact is important to the contraction rules of Appendix A. If one changes X to X' inside M^n by an elementary move like that of Fig. 40, then the regular neighborhoods $N(X, M^n)$ and $N(X', M^n)$ are homeomorphic in a more or less unique and canonical way. Moves like that of Fig. 40 are called "duality transformations" in classical DTU (also in dual resonance models) and "Whitehead moves" in topology.

For any surface pair (Σ_Q, Σ_C) the belt $\partial\Sigma_C = \Sigma_C \cap \Sigma_Q$ has a well-defined regular neighborhood $N(\partial\Sigma_C; \Sigma_Q)$ which we call the thickened belt and denote by $th(\partial\Sigma_C)$. It is, of course, always orientable. The information contained in $th(\partial\Sigma_C)$ is an ordering of the belt graph analogous to the ordering of the Landau graph (Appendix A).

III. The 3-dimensional thickenings of a smooth surface S are just the line bundles E of basis S (see Appendix A of Ref. 14).

IV. The above examples show that, in general, n-dimensional thickenings of a given X are not unique. It furthermore may happen, for a given dimension $n > \dim X$, that X fails to admit any n-dimensional thickening. Consider for example an annulus A and a Möbius ribbon M with embedded loops Γ and Γ' as shown in Fig. 41. If

$$X = \{A \cup M, \text{ with } \Gamma \text{ glued to } \Gamma'\}$$

then X does not admit any 3-dimensional thickening.

4. Landau graph and glitches

A classical surface Σ_C within a topological index $\tau = (\Sigma_Q, \Sigma_C)$ houses a Landau graph L as well as HR arcs and charge arcs. Connected sums of surface pairs are accompanied by sums of the Landau graphs and also of the HR arcs and charge arcs; the ensemble of connections is a "Landau connected sum". A variety of general features of any "admissable" surface pair may be deduced by induction from the requirement that any admissable τ be obtainable from our a priori-defined "zero-entropy" pairs through Landau connected sums followed by specified contractions. The contraction rules for L are given in Appendix A. The rules for HR arcs and junction lines, given in the

main text, state that any closed HR loop within a single patch of Σ_C is to be erased, as is any closed junction line uncut by a Landau arc where a single-patch sphere cuts a plane equatorially (the sphere also disappears). Each charge arc connecting peripheral triangles runs "parallel" to the associated HR arc and obeys the same contraction rules; each core charge arc obeys the same contraction rules as the associated junction line. The deducible general features of any τ are:

a) HR arcs touch neither charge arcs nor L nor junction lines (HR arcs lie along the belt, joining adjacent belt segments from different particle pieces.)

b) The "ends" of L, $\partial L = L \cap \partial \Sigma_C$, do not touch junction lines (or core charge arcs).

c) Although at zero entropy L is entirely on one sheet (together with all core charge arcs), certain connected sums lead to glitches where L crosses a junction line (Sec. IV, main text) as well as crossing the associated core charge arc. L never touches the end of a junction line (or the end of a charge arc).

d) Any sheet of Σ_C housing a portion of L contains at least one Landau vertex on each connected piece of L. (Trivial Landau vertices may occur). Contraction of L never moves a Landau vertex out of its smooth sheet across a junction line (Appendix A).

If the total number of glitches within some Σ_C is $\gamma(\Sigma_C)$, it follows from the foregoing that

$$\gamma(\Sigma_{C'} \# \Sigma_{C''}) \geq \gamma(\Sigma_{C'}) + \gamma(\Sigma_{C''}) \qquad (B.5)$$

That is, a baryon plug may produce a new glitch, but glitches once present cannot be removed through a contraction following any Landau connected sum. Loosely speaking. a Landau graph that once enters some sheet of Σ_C remains forever tied to that sheet by a Landau vertex.

5. Twisted diquark plugs

When does a baryon plug generate a glitch? An elementary-particle disk not only houses an end of a Landau graph, but electric charge and edge flavor are attached to the quark triangles. Suppose that an intermediate baryon contains 3 different flavors, say u,d,s. As explained in Sec. VIII of the main text, there are 6 different plugs to consider--corresponding to the six permutations of the 3 flavors as shown in Fig. 42. Only the identity permutation fails to increase entropy. The other five permutations are characterized as "switches" in Sec. VIII. Cyclic permutations lead to glitches, but apart from the required displacement of the Landau graph, any cyclic quark permutation allows the entire "in" baryon disk to be "turned over" and superposed on the "out" baryon disk. A plug corresponding to an odd permutation of quarks cannot be so directly accomplished; here some quark triangles must be plugged independently.

If the odd permutation interchanges the two triangles not touched by the Landau graph, we characterize the plug as a "diquark twist" or simply as a "twist". The two other odd permutations correspond to a twist together with a glitch. It suffices then to describe the simple twist. Our description will also be appropriate to baryonium plugs with one or two diquark twists (Sec. VIII main text).

Refering to the example of Fig. 42, the simple diquark twist corresponds to a permutation of the u and d quarks, with the s quark remaining in contact with the Landau graph. As a

first step let us plug the 2-triangle disks that contain the core triangle and the s quark. We arrive at an intermediate surface pair and thence proceed to two further plugs--of "in" u quark to "out" u quark and "in" d quark to "out" d quark. The result of these three consecutive plugs is the same as if we had made simple plugs to a "twisted" baryon propagator:

$$\tau = \tau' \# \tau'' = \tau' \# [\text{twisted } (B_{in}, B_{out})\text{propagator}, \tau_1] \# \tau'' \quad (B.6)$$

diquark twist; simple plug; simple plug

The twisted propagator $\tau_1 = (\Sigma_Q^1, \Sigma_C^1)$ is as follows:

α) Σ_Q^1 is a torus covered by the B_{in}, B_{out} disks of Fig. 42 with all six of the nontrivial vertices (marked by heavy dots) identified. This torus is obtained from the bounded, genus-2, surface of Fig. 43 by crushing the entire boundary to a single point--the just-described nontrivial vertex of the Σ_Q^1 triangulation. Note that Σ_Q^1 is the nonplanar orientable thickening of the corresponding belt.

β) The classical surface Σ_C^1 is obtained by joining the u, d sheets of Fig. 44(a) in such a way as to create a Möbius band [Fig. 44(b)]. The boundary of Σ_C^1 is the belt shown in Fig. 43. It follows that $g(\Sigma_C^1) = 1$, so the diquark twist increases entropy.

6. Entropy Theory

The following list of 4 entropy indices has been identified:

$$g(\Sigma_C),\ p(\Sigma_C) - 1,\ j(\Sigma_C) - 1,\ \text{and } \gamma(\Sigma_C), \quad (B.7)$$

accounting, respectively, for genus, classical patches, boundary structure and glitches. Each index has the entropy property either in the strong form

$$i(\tau' \# \tau'') \geq i(\tau') + i(\tau'')$$

or at least in the weak form

$$i(\tau' \# \tau'') \geq \max\left(i(\tau'), i(\tau'')\right)$$

The following claims are easy to check:

I. Consider all "admissable" surface pairs (Σ_Q, Σ_C) obtained by connected sum from our a priori defined "zero-entropy" pairs. Then any admissable (Σ_Q, Σ_C) with all four indices Eq. (B.7) equal to zero is of zero entropy.

II. A zero-entropy surface pair cannot be obtained from a Landau connected sum of admissable surfaces pairs τ', τ'' if either ingredient is of nonzero entropy.

III. Moreover, any splitting $\tau = \tau' \# \tau''$, where τ is zero entropy, implies that τ' and τ'' are admissable and hence zero entropy. (The concept of ordered S matrix, introduced in Sec. V of the main text, rests on requirements II and III.)

IV. Fixing the values of the four indices (B.7) determines an admissable surface pair up to finitely many possible choices.

V. Our indices are intrinsically defined, independently of the way that $\tau = (\Sigma_Q, \Sigma_C)$ has been obtained from zero entropy. The indices are "natural"--making sense in a purely topological context.

There is of course no claim that (B.7) is the only possible list of entropy indices meeting requirements I → V. In fact we now proceed to describe an alternative list of 5 indices.

The thickened Landau graph th(L) described in Sec. VIII of the main text can be used conveniently to record the entropy history of $\tau(\Sigma_Q, \Sigma_C)$. or each τ there is a well-defined th(L) on which we can record, in a natural fashion, 0-P patching as in Fig. 45(a) glitches as in Fig. 45(b) and twists as in Fig. 45(c), with the understanding that

i) glitches, twists and patch boundaries do not commute,

ii) neither switches (glitches or twists) nor patch boundaries may be slid past a Landau vertex,

iii) each Landau vertex has a definite 0-P character (Appendix A),

iv) a thickened Landau-arc segment between two successive Landau vertices carries at most one switch and at most one patch boundary (if both switches and patching are absent the segment can be contracted to a point).

The embellished thickened Landau graph (which we still denote by th(L)) completely determines the surface pair (Σ_Q, Σ_C) and hence the set of four entropy indices $g(\Sigma_C)$, $p(\Sigma_C)$, $j(\Sigma_C) = g(\Sigma_C) + b(\Sigma_C)$ and $\gamma(\Sigma_C)$. So far as $p(\Sigma_C)$ and $\gamma(\Sigma_C)$ are concerned, this fact is evident since the embellishment of th(L) records 0-P patching and glitches.

How can one reconstruct the whole (Σ_Q, Σ_C) from its th(L)? Remember that th(L) contains the contracted Landau graph L and hence can be divided unambiguously into pieces each containing exactly one Landau vertex v_1:*

$$\text{th(L)} = \text{th}(L^1) \# \text{th}(L^2) \# \ldots \qquad \text{(B.8)}$$

* The total number of Landau vertices satisfies the weak entropy property.

It is understood that all the 0-P division lines, glitch and twist markings occur at the # signs. There is furthermore a decomposition

$$(\Sigma_Q, \Sigma_C) = (\Sigma_Q^1, \Sigma_C^1) \# (\Sigma_Q^2, \Sigma_C^2) \# \ldots \qquad \text{(B.9)}$$

which parallels Eq. (B.8) and such that Σ_C^i contains L^i. One obtains the connected (Σ_Q^i, Σ_C^i) surface pairs by taking a set of zero-entropy surfaces that builds up (Σ_Q, Σ_C), performing all plugs that do not involve 0-P transitions, glitches or twists, and then making all the necessary contractions. The object $\text{th}(L^i)$ is the thickened Landau graph corresponding to (Σ_Q^i, Σ_C^i) and we claim that it determines (Σ_Q^i, Σ_C^i).

Indeed Σ_C^i has only one patch, no glitches and only one Landau vertex v_i, with L^i living on a "main sheet". Also Σ_Q^i has been built without twists. So clearly

$$p(\Sigma_C^i) = 1,\ \gamma(\Sigma_C^i) = 0,\ g(\Sigma_C^i) = g(\text{th}(L^i)),\ b(\Sigma_C^i) = b(\text{th}(L^i)).$$

For all practical purposes Σ_C^i is like a classical-DTU bounded smooth surface. Topologically speaking, this surface is the {main sheet of Σ_C^i}, homeomorphic to {th(L), without embellishments}. This Σ_C^i can be supplemented with a Σ_Q^i built out of spheres as in classical DTU.

Once the (Σ_Q^i, Σ_C^i)'s are determined, Formula (B.8) tells us exactly how to perform the plugs in Formula (B.9), because the embellishments record exactly the whole story of 0-P transitions, glitches and twists. It follows that th(L) determines (Σ_Q, Σ_C).

How can one compute directly $g(\Sigma_C)$ and $b(\Sigma_C)$ (hence $j(\Sigma_C)$) from th(L)? Assume for the moment that there are no twists. Σ_C does not house th(L) but it contains L and retracts on L (if L is contracted).

Hence it retracts on the possibly non-orientable smooth thickening of L contained in Σ_C, which we denote $\overline{th}(L)$. So $g(\Sigma_C) = g(\overline{th}(L))$. The object $\overline{th}(L)$ can be determined from the embellished th(L): one takes L with the same ordering as for th(L) but one makes the thickening along a closed circuit orientable or not according to whether the number of glitches along the circuit is even or odd. In the general case with twists it is easy to show that

$$g(\Sigma_C) = g(\overline{th}(L)) + \{\text{number of twists}\}.$$

One first cuts along the twists, applies the special case above, and then glues back to restore the twists.

If th(L) is embellished with quark lines, $b(\Sigma_C)$ is determined in the following way. The ends of L correspond exactly to the external particles which fill the belt $\partial\Sigma_C$ according to two rules:

(1) Two (external) particles on the ends of the same quark line belong to the same component of $\partial\Sigma_C$.

(2) Quark lines attached to the same (external) particle belong to the same component of $\partial\Sigma_C$.

These two rules allow us to divide unambiguously the ends of L into boundary components of $\partial\Sigma_C$.

APPENDIX C: PATCHWISE-ORIENTED SURFACES

A patchwise-oriented surface S is, by definition, a usual surface divided into 2-dimensional regions of disjoined interiors called "patches", such that:

i) Each patch is oriented,

ii) Two adjacent patches have always opposite orientations so that they induce the same orientation of any common edge, as in Fig. 46.

This definition makes sense for surfaces with or without boundary and extends without trouble to any dimension. If S is orientable and globally oriented the orientation of a particular patch may agree or may disagree with the global orientation. When in the main text we have described a quantum triangle orientation as "clockwise" ("anticlockwise"), what was meant is that the patch orientation agrees (disagrees) with the global orientation.

One can easily show that any surface (more generally, any n-manifold), whether orientable or not, can be patchwise oriented in many ways. For example, two possible ways to patchwise orient a triangular disk are shown in Fig. 47. We have employed the scheme of Fig. 47(a) in our theory but not the scheme Fig. 47(b), because of contraction considerations. The possibility of patchwise orienting nonorientable surfaces means that a significance for orientation reversal does not require global orientability.

APPENDIX D: TOPOLOGICAL M FUNCTIONS; Zero-Entropy Spin Dependence and P, C, T

S-matrix connected parts in the absence of spin are analytic functions of particle momenta, apart from isolated singularities described by Landau-graphical rules (Appendix A and Ref. 1. In the presence of spin, Landau rules continue to have their spinless form if understood as applying to M functions,[1, 17] whose spin indices in changes of Lorentz frame of reference transform independently of the values of momenta. An M function is not immediately equal to an S-matrix connected part but is related thereto by a well-defined momentum-dependent spin-index tranformation.[1, 17] The advantage of M functions is exemplified by the principles of crossing and TCP invariance. Let an M function for an N-particle event be labeled $M_{\alpha_1,\ldots,\alpha_N}(p_1 t_1,\ldots,p_N t_N)$, where the $p_k = (E_k, \vec{p}_k)$ are energy-momentum four vectors, the t_k designate particle types (e.g., t_1 = proton, t_2 = positive pion ...), and the α_k are spinor indices whose essential property is that their behavior in a Lorentz transformation is controlled entirely by the 6 parameters (rotation and boost) labeling the Lorentz-group element. The crossing principle states that the complex momentum space of a single analytic M function contains nonoverlapping physical regions in all of which the p_k are real but each of which belongs to a distinct collection of signs $\eta_k = \pm$ for the E_k. The usual convention, which we adopt, is that if $\eta_k = +$ (-) the k'th particle is outgoing (ingoing) with physical energy-momentum $p_k(-p_k)$. The physical interpretation of the type-indices t_k and the spinor indices α_k obeys a similar rule: For example if a certain value of t_k designates "proton"

for $\eta_k = +$ then the same value of t_k means "antiproton" when $\eta_k = -$. If a certain value of α_k means $s_z = +1/2$ for $\eta_k = +$ then the same value of α_k means $s_z = -1/2$ for $\eta_k = -$. An M function is invariant if a proper complex Lorentz transformation is applied to all p_k and all α_k. One such transformation turns out to change each p_k to $-p_k$ while leaving untouched the α_k; this transformation is equivalent to the product of time reversal (T), parity (P) and particle-antiparticle conjugation (C). Invariance under CPT is thus an automatic property of any M function.

A topological M function ${}^{\tau}M^{\kappa}_{\alpha_1,\ldots\alpha_N}(p_1,\ldots,p_N)$ lacks particle-type indices but instead carries the topological index τ and the order index κ described in the main text. The topological expansion of an elementary connected part now reads

$$M_{\alpha_1,\ldots,\alpha_N}(p_1, t_1\ldots,p_N, t_N) = \sum_{\tau(t_1\ldots t_N),\,\kappa} {}^{\tau}M^{\kappa}_{\alpha_1,\ldots\alpha_N}(p_1,\ldots,p_N) \tag{D.1}$$

where by $\tau(t_1\ldots t_N)$ we mean that each surface pair within the sum contains N quantum discs appropriate to the elementary particle types $t_1\ldots t_N$. Apart from spin degeneracy each elementary particle corresponds to a distinct and different collection of oriented triangles, each with an attached oriented (charge) arc and with separate (edge flavor) orientations for those edges building the particle-disk perimeter. The order index κ attaches each (p_k, α_k) to a particular quantum disk compatible with the particle type.

Each elementary-particle spin index α_k is actually a collection of 2-valued indices belonging to (0, 1/2) or (1/2, 0) spinor representations of the Lorentz group. This idea, stemming from Stapp's original 1962 M-function paper,[17] was associated with HR graphs by Mandelstam in 1970.[18] HR arcs are attached to peripheral triangles of particle disks, and Mandelstam's scheme is equivalent to attaching one 2-valued spinor index to each peripheral triangle. Thus elementary mesons carry two spinor indices, elementary baryons carry 3 spinor indices and elementary baryoniums carry 4 spinor indices. It is furthermore natural and convenient to agree that the physical spin significance of a spinor index attached to a counterclockwise peripheral triangle is the negative of that for an index attached to a clockwise triangle, because counter-clockwise peripheral triangles are always matched with clockwise both in contractions and in Landau connected sums. Our rule for the dependence of zero-entropy M functions on spinor indices employs this convention.

The rule is the same as that of Stapp,[4] although we express it differently. Any HR arc joins two mated peripheral triangles, so we associate with each HR arc the pair of spinor indices coming from its triangle pair. As explained in Stapp's paper, a spin index may appear in one of four different types: upper dotted, lower dotted, upper undotted and lower undotted. Each type transforms in a distinct and well-defined way under a Lorentz transformation [Eq. (2.9) of Ref. 4]. It is purely a matter of convenience which type of index is attached to an M function, the connection always being well defined between M

functions with different index types.* We adopt the rule that, between the two indices belonging to the same HR arc, one index is upper and one lower according to the sense of the patch orientation (not the sense of the HR arc). We shall consistently associate the lower index with the "front" particle (following the patch arrow; see Fig. 48) of the pair connected by the HR arc.

With the foregoing conventions the Stapp spin dependence for zero-entropy M functions is simply a product of Kronecker delta functions, one for each HR arc; the momentum-dependence resides in a separate factor. Figure 48 gives an example. Provided the conventions are consistently followed one may then at zero entropy associate a single spin-index value, like a flavor-index value, to each HR arc. This rule may not be used when ortho↔para transitions occur.

What determines whether the Kronecker-delta function belonging to a given quark line carries dotted or undotted indices? This important question we do not resolve in the present paper. Given the fact that a quark line effectively carries a flavor label and that at zero entropy it also carries a (1,2,3) "topological color" label, we can assign to each flavor-color combination either dotted or undotted indices in the ortho case, with the opposite assignment in the para case. The Stapp spin dependence has the essential property of transitivity (self-reproducing) in zero-entropy connected sums. This property is transparent once it is established that the connection between M functions and S-matrix elements implies M-function

* Tranformation between dotted and undotted indices depends on the velocity of the associated particle.[17]

"spin propagators" in Landau products that are of the same Kronecker-delta form as the ortho and para zero-entropy propagators. We refer the reader here to the Appendix of Iagolnitzer's book.[1]

The parity operation on spin indices changes upper to lower and dotted to undotted, or vice versa,[17] so that Stapp's zero-entropy form associates the parity operation P with classical-patch orientation inversion ($I_{c\ell}$) in the following sense:

$$P\ {}^{\tau}M^{\kappa}_{\alpha_1,\ldots,\alpha_N}(p_1,\ldots,p_N) \equiv {}^{\tau}M^{\kappa}_{P\alpha_1,\ldots,P\alpha_N}(Pp_1,\ldots,Pp_N)$$

$$= I_{c\ell}\,{}^{\tau}M^{\kappa}_{\alpha_1,\ldots,\alpha_N}(p_1,\ldots,p_N), \qquad (D.2)$$

where $Pp_k = (E_k, -\vec{p}_k)$. The zero-entropy momentum dependence resides in a separate factor which, by Lorentz invariance, can only depend on scalar products $p_i p_j$ of momenta. Since such products are automatically invariant under the parity operation it is natural that this scalar factor be the same for ortho and for para. The one-to-one matching of ortho and para zero-entropy topologies then assures parity invariance for strong interactions.

The C operation of particle-antiparticle conjugation similarly has been shown by Stapp to correspond to simultaneous inversion of <u>all</u> orientations, both quantum and classical. That is

$$C\ {}^{\tau}M^{\kappa}_{\alpha_1,\ldots,\alpha_N}(p_1,\ldots,p_N) = {}^{C\tau}M^{\kappa}_{\alpha_1,\ldots,\alpha_N}(p_1,\ldots,p_N), \qquad (D.3)$$

where

$$C\tau = (I_{c\ell} \times I_Q)\tau$$

with

$$I_Q \equiv I_{HR} \otimes I_{ch} \otimes I_{f\ell}. \qquad (D.4)$$

The symbols I_{HR} and I_{ch} refer to quantum patch and charge orientations, respectively. (A global inversion of one of these two orientations without inverting the other is never allowed because for core triangles these orientations must agree.) The symbol $I_{f\ell}$ refers to quark edge (flavor) orientation. The C operation does not change ortho to para but reverses the sign of all internal quantum numbers. It is consistent and natural to postulate at zero entropy that the scalar factor belonging to any (τ,κ) has the same value as that belonging to $(C\tau,\kappa)$, thereby assuring C invariance for strong interactions.

From TCP invariance it may be inferred that

$$T\ {}^{\tau}M^{\kappa}_{\alpha_1\ldots\alpha_N}(p_1\ldots p_N) = {}^{I_Q\tau}M^{\kappa}_{\alpha_1\ldots\alpha_N}(p_1\ldots p_N). \qquad (D.5)$$

Although time reversal does interchange ortho and para, an ortho $\to$ para <u>transition</u> remains ortho $\to$ para and similarly for para $\to$ ortho. It can be shown[14] that such transitions may be interpreted as quark coupling to right-handed or left-handed "currents". Thus, as expected, right-handed transitions remain right-handed under time reversal and left-handed transitions remain left-handed.

The unresolved issue of how to associate dotted and undotted spinor indices with flavor-color combinations has the potential of breaking the flavor symmetry inherent in zero entropy (Sec. X). This important matter will be discussed elsewhere.

ACKNOWLEDGMENTS

Lengthy consultations with J. Finkelstein, B. Nicolescu, H. P. Stapp, G. Veneziano and G. Weissmann have made major contributions to this paper. Also of help have been discussions with L. Balazs, R. N. Cahn, F. Capra, H. M. Chan, E. Jones, M. Levinson, R. McMurray, S. Mandelstam, C. Rosenzweig, J. P. Sursock, J. Uschersohn, R. Vinh-Mau and C. N. Yang. One of the authors (G.F.C.) wishes to thank the CERN Theory Division for hospitality and support during the initial stages of this work. This work was supported by the Director, Office of Energy Research, Office of High Energy and Nuclear Physics, Division of High Energy Physics of the U.S. Department of Energy under Contract No. W-7405-ENG-48.

REFERENCES

1. D. Iagnolitzer, The S Matrix, North Holland, Amsterdam (1978).
2. H. Harari, Phys. Rev. Letters 22, 562 (1969). J. Rosner, Phys. Rev. Letters 22, 689 (1969).
3. G.F. Chew and C. Rosenzweig, Phys. Reports 41C, #5 May 1978.
4. H.P. Stapp, Spins and Baryons in the Topological Expansion, Lawrence Berkeley Laboratory preprint LBL-10774, April 1980.
5. G.F. Chew and V. Poénaru, Phys. Rev. Letters 45, 229 (1980).
6. G. Veneziano, Nuc. Phys. B74 (1974) 365; Phys. Letters 52B (1974) 220.
7. M. Ciafaloni, G. Marchesini, G. Veneziano Nucl. Phys. B98 (1975) 472, 493.
8. G. Weissmann, International Journal of Theoretical Physics, 17 No. 11 (1978) p. 853.
9. M. Levinson, private communication, Berkeley (1980).
10. G.C. Rossi and G. Veneziano, Nucl. Phys. B123 (1977) 507; K. Konishi, Nucl. Phys. B131 (1977) 143; H.P. Stapp, Nuovo Cim. 46A (1978) 37; F. J. Capra, Phys. Lett. 68B (1977) 93.
11. G.F. Chew, J. Finkelstein, J.P. Sursock, G. Weissmann, Nucl. Phys. B136 (1978) 493.
12. J.P. Sursock, Nuclear Physics B145 (1978) 166.
13. G.F. Chew, Nucl. Phys. B151 (1979) 237.
14. G.F. Chew, J. Finkelstein, R.E. McMurray, Jr., and V. Poénaru, Physics Letters 100B, 53 (1981); LBL-11435, submitted to Physical Review.

15. P. Gauron, B. Nicolescu and S. Ouvry, Orsay preprint IPNO/TH 80/53 (1980).

16. For a list of glueball references, see M. Chanowitz, LBL-11977 (1980).

17. H. P. Stapp, Phys. Rev. 125, 2139 (1962).

18. S. Mandelstam, Phys. Rev. D1, 1745 (1970).

FIGURE CAPTIONS

1. Nonordered vertex corresponding to a 4-particle physical connected part.
2. Planar (single-boundary) classical surface for a topological component of the physical amplitude of Figure 1.
3. Cylindrical (2-boundary) classical surface for a topological component of the physical amplitude of Figure 1.
4. Toroidal (single boundary) classical surface for a topological component of the physical amplitude of Figure 1.
5. (a) Nonordered Landau graph associated with a singularity of the physical amplitude of Figure 1.
   (b) Ordered Landau graph corresponding to one of the topological components of the singularity graph of Figure 5(a).
6. The classical surface of Figure 2 with embedded HR arcs.
7. The contraction of two adjacent (C,D) meson pieces of classical-surface boundary to a single meson piece. The C-meson piece extends from vertex #1 to vertex #3 while the D-meson piece extends from vertex #3 to vertex #5. (All vertices are trivial.) The contraction forms and then erases a closed HR loop. Not shown but easily inferred is the corresponding Landau-graph contraction (Appendix A) which replaces two "parallel" meson arcs by a single arc.
8. Intersection of three sheets of Σ_C at a junction line. In this example the boundary of one sheet, which happens to be interrupted only by the single (exhibited) junction line, is shown in its entirety. The boundaries of the other two sheets, left incomplete in the figure, might be interrupted by further junction lines.

The oriented lines attached to the belt are HR arcs.

9. The four elementary-hadron belt pieces allowed by the zero-entropy bootstrap (see Sec. V):
   (a) meson
   (b) "out" (E > 0) baryon or "in" (E < 0) antibaryon (see Appendix D)
   (c) "out" (E > 0) antibaryon or "in" (E < 0) baryon
   (d) baryonium
10. (a) HR-oriented belt-graph for a (zero-entropy) 4-particle connected part (two baryons, one meson and one baryonium). Dotted lines are HR arcs.
    (b) Separation of this belt graph into particle pieces.
11. Three types of glitches: (a) ortho (b) para (c) ortho-para transition.
12. A 2-bead "twisted" belt graph belonging to a Σ_C of nonzero entropy. In Appendix B it is shown that the classical surface here has only 4 sheets, rather than the 5 associated with the untwisted belt of Fig. 10(a). The "disquark twist" has united the two inert sheets of one bead.
13. "Elementary-particle" quantum disks corresponding to the belt pieces of Fig. 9.
14. Contraction (erasure) of two adjacent matching disks on Σ_Q.
15. A 2-meson (A,C) channel disk.
16. Contraction of the Fig. 15 channel disk to a single-particle disk.
17. Harari-Rosner diagram of the contraction from Fig. 15 to Fig. 16.
18. Division of a Σ_Q sphere into 4 patches by lunar insertion.
19. (a) Core triangle on Σ_Q.

    (b) Peripheral triangle on Σ_Q.
20. Trivial vertices of the Σ_Q triangulation belonging to Fig. 10, shown along the belt graph. Notice the correspondence between Σ_Q trivial vertices and HR arcs on Σ_C; either delineate the elementary particles.
21. The Σ_Q triangulation correspondings to Figs. 10 and 20.
22. Patch orientations of baryon disks.
23. Belt patterns if Σ_Q were divided into squares.
24. The four edge flavors (and antiflavors).
25. Thickened Landau graph for the topology of Figs. 10, 20, and 21. The dashed lines are core charge arcs while the dotted lines are HR arcs.
26. Thickened baryon Landau arc when the core charge arc is replaced by a pair of quark lines (antidiquark).
    (a) Clockwise HR orientation.
    (b) Anti-clockwise HR orientation.
27. The three topological colors.
28. Switches along a baryon Landau arc.
29. Switches along a baryonium Landau arc.
30. Connected sum of zero-enthropy τ's that corresponds to meson decay of baryonium. Dashed lines are core charge arcs while dotted are HR arcs.
31. Spin-flavor labels attached to the quarks and antiquarks of a baryonium disk.
32. Examples of forbidden and allowed ordinary Landau graphs.
33. Examples of equivalence between ordered Landau graphs.
34. Examples of contractions leading to trivial Landau vertices.

35. Four categories of connected sums.

36. Singularities of the quantum surface.

37. A single-vertex, 2-arc graph.

38. The 8 distinct thickenings of the graph of Fig. 37.

39. Commutative diagram representing equivalence of two thickenings A and A'.

40. Example of a "Whitehead move" or "duality transformation".

41. Example of a "space" that admits no thickening: The annulus A and Möbius band M are glued along the loops Γ and Γ'.

42. The six different quark permutations that may occur in a baryon plug.

43. Thickening of the belt belonging to a baryon "propagator" for a diquark twist.

44. (a) Σ_C for the zero-entropy (identity-permutation) baryon propagator corresponding to Fig. 42.

    (b) Σ_C for a diquark-twist baryon propagator.

45. A notation for recording complexity on th(L): Dashed lines are core charge arcs, dotted lines are HR arcs.

    (a) Ortho-para transition.

    (b) Glitch

    (c) Diquark twist

46. A patchwise-oriented disk.

47. Two ways of patchwise orienting a triangular disk.

48. Example of Stapp's zero-entropy spin dependence for a 3-meson connected part. The central arrow indicates the classical patch orientation.

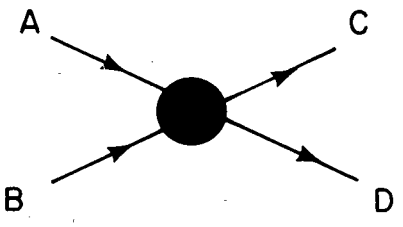

XBL 802-204

Figure 1

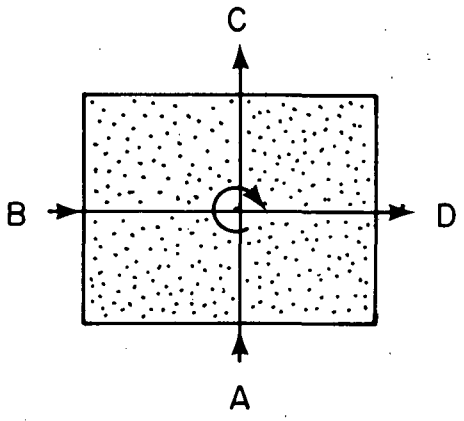

XBL 802-205

Figure 2

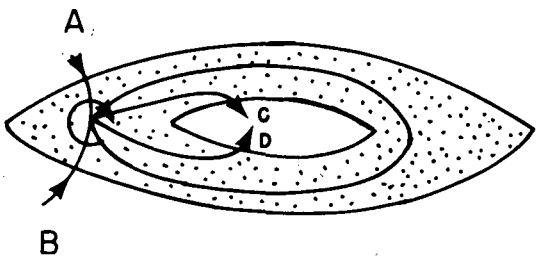

XBL802-206

Figure 3

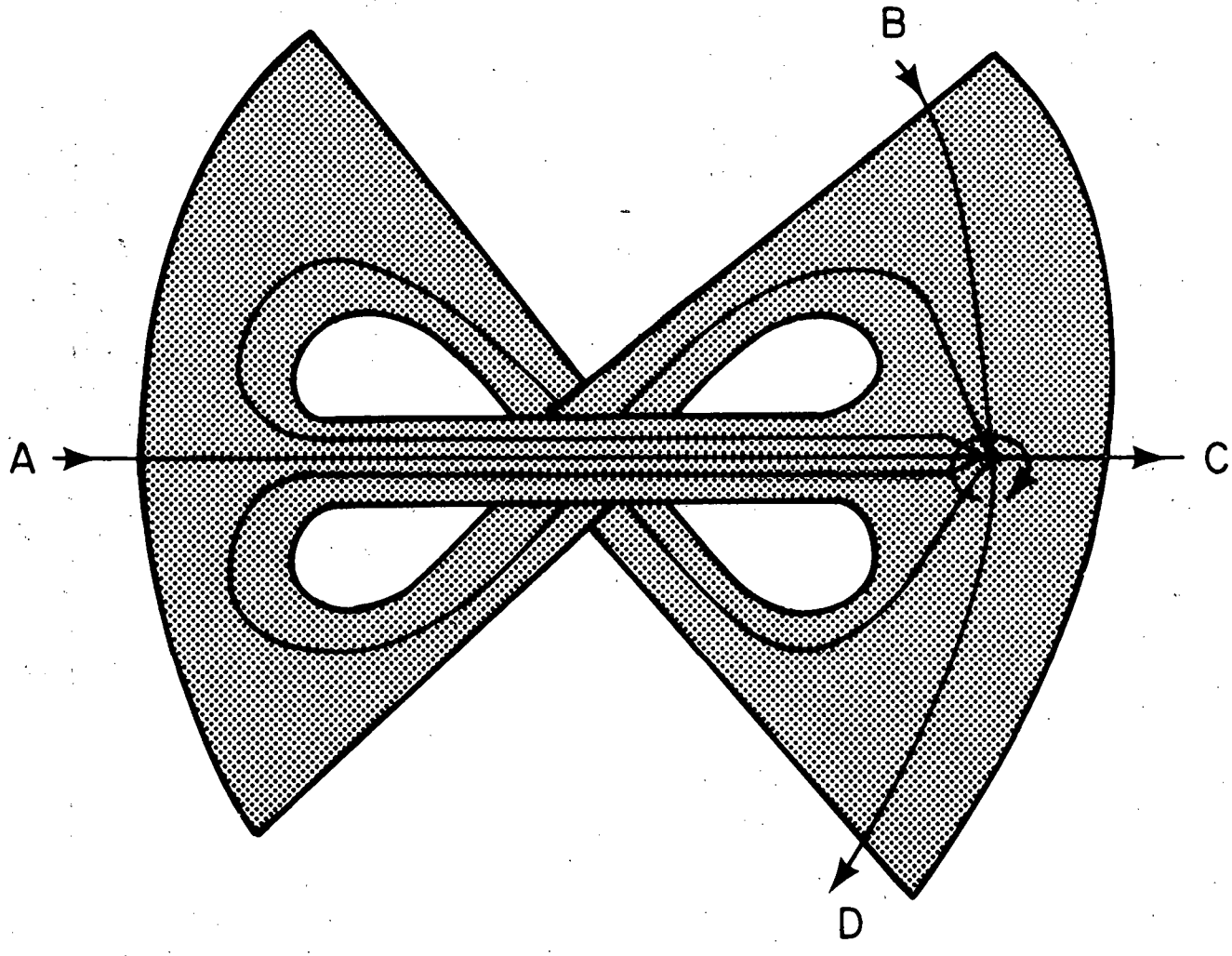

Figure 4

XBL 802-200

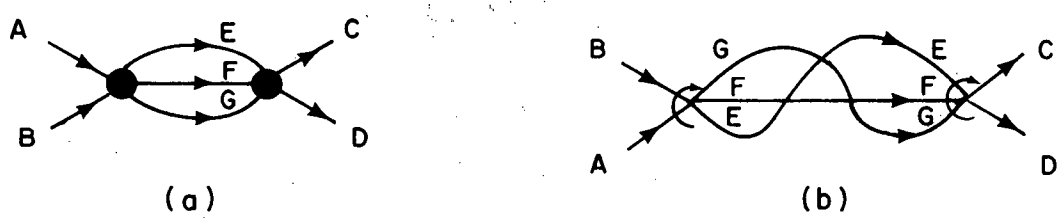

Figure 5

XBL802-207

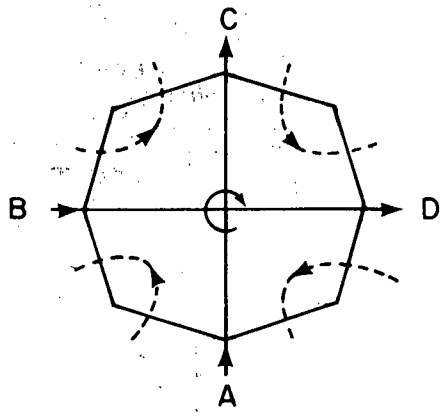

XBL802-208

Figure 6

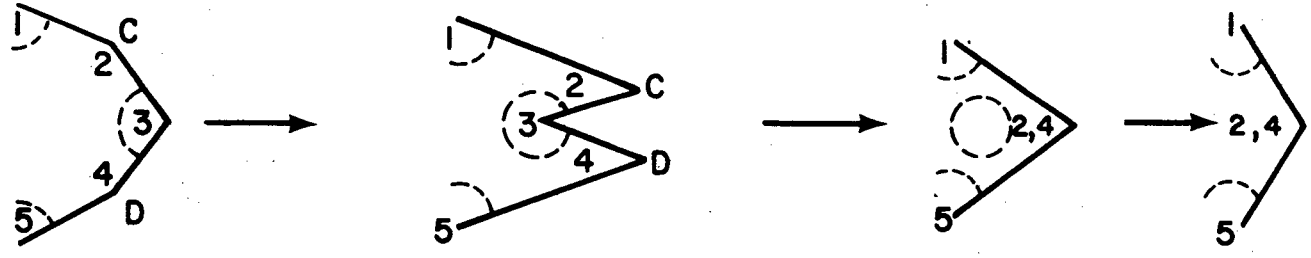

XBL 814-720

Figure 7

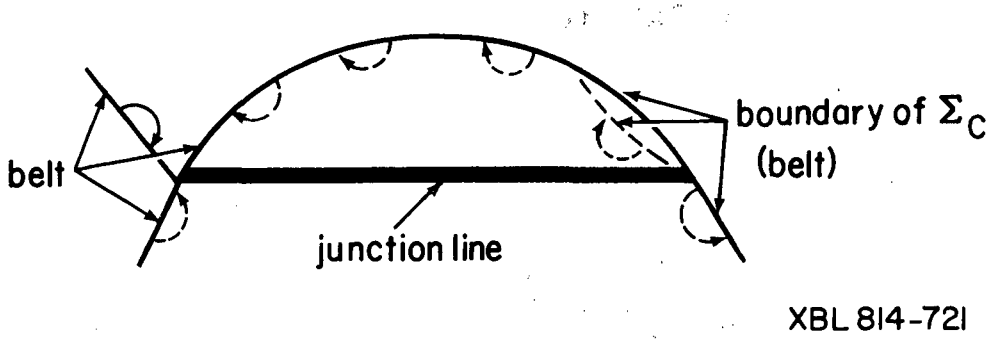

Figure 8

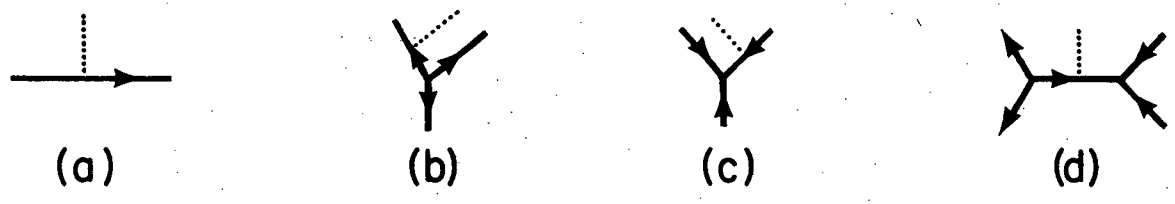

XBL 814-722

Figure 9

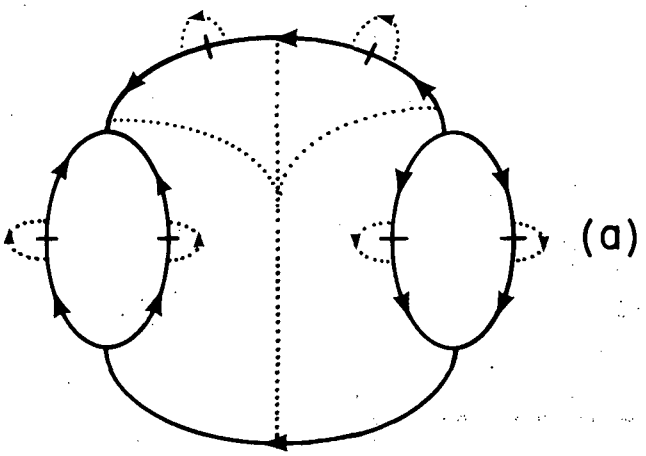

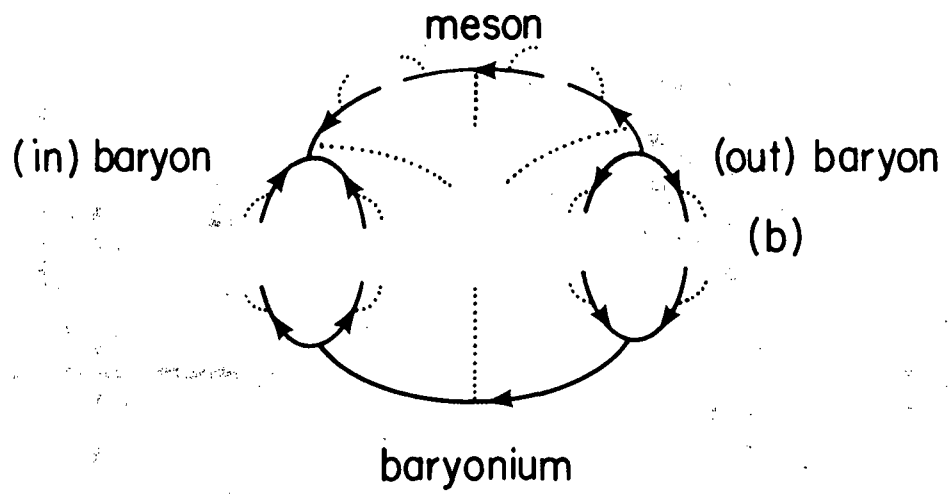

XBL 814-723

Figure 10

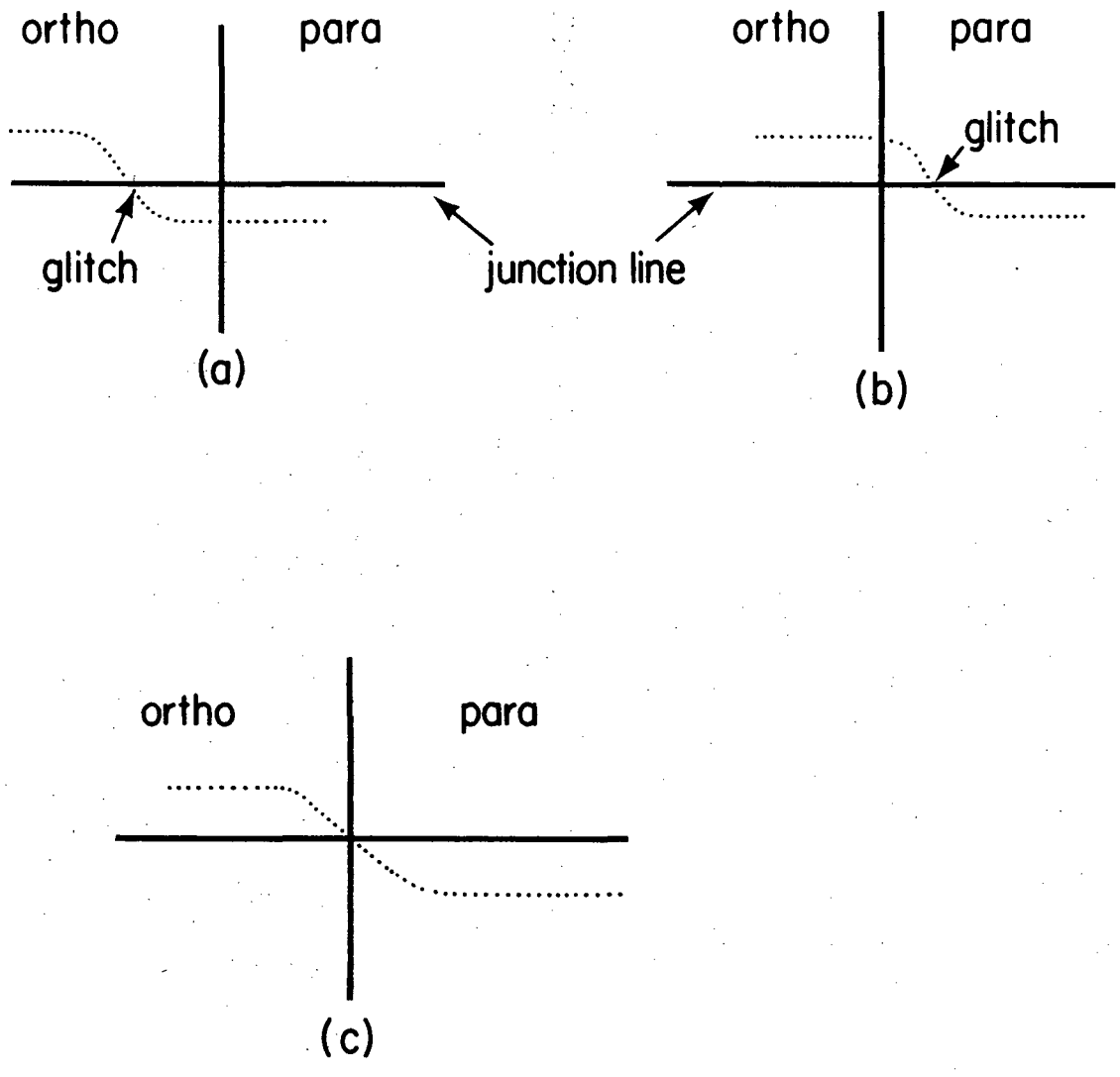

XBL 814-724

Figure 11

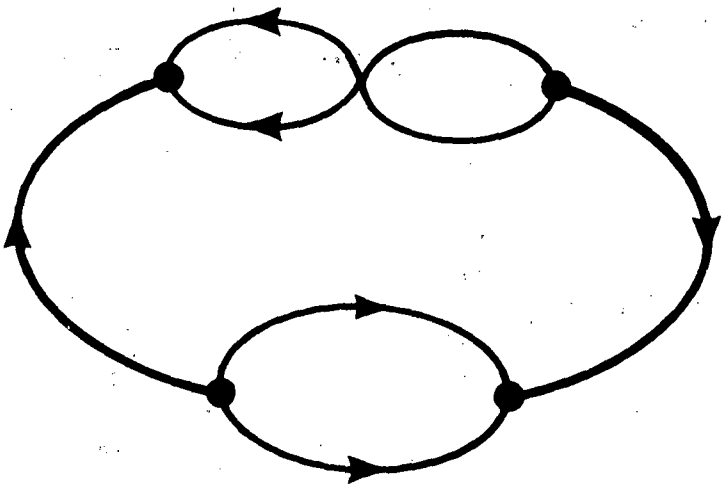

XBL 814-725

Figure 12

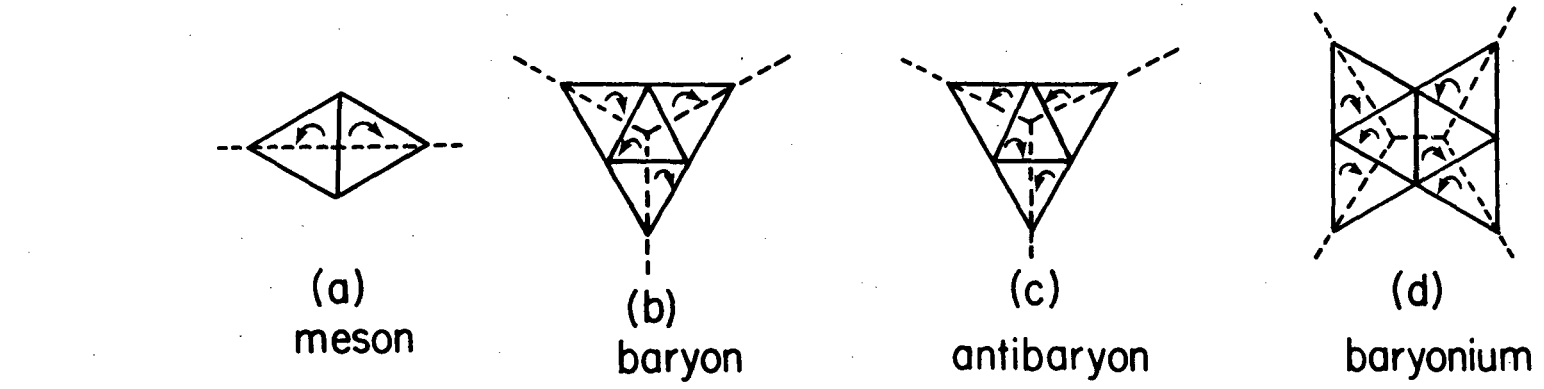

Figure 13

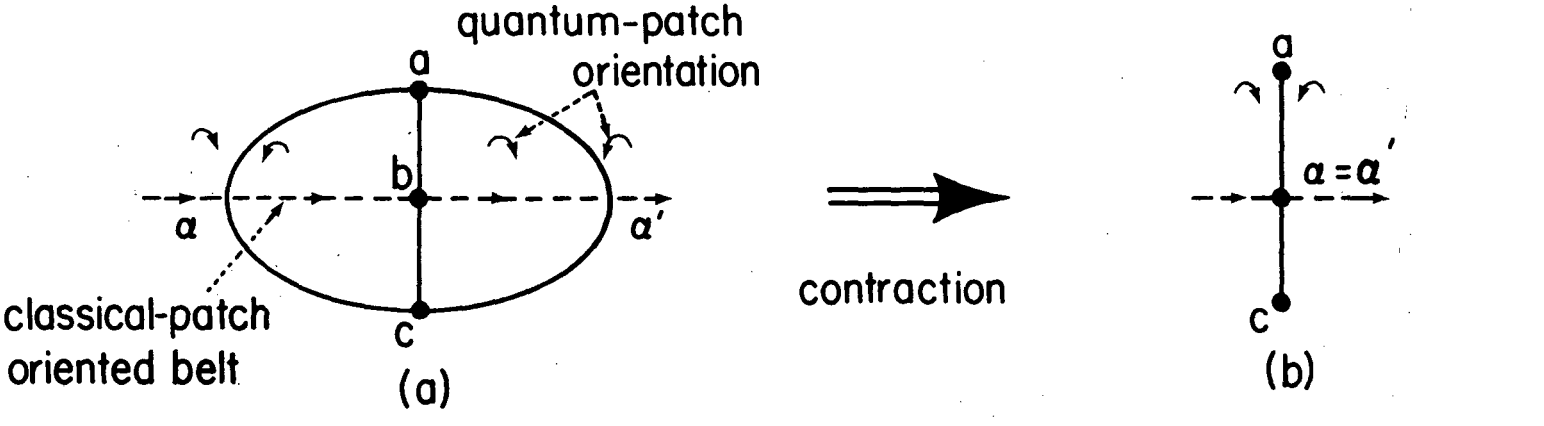

Figure 14

XBL814-726

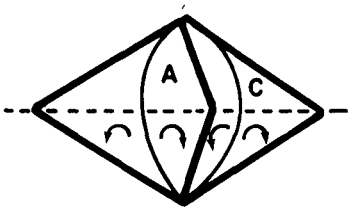

XBL 802-217

Figure 15

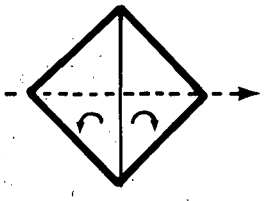

XBL 802-218

Figure 16

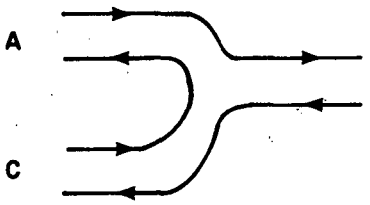

XBL 802-219

Figure 17

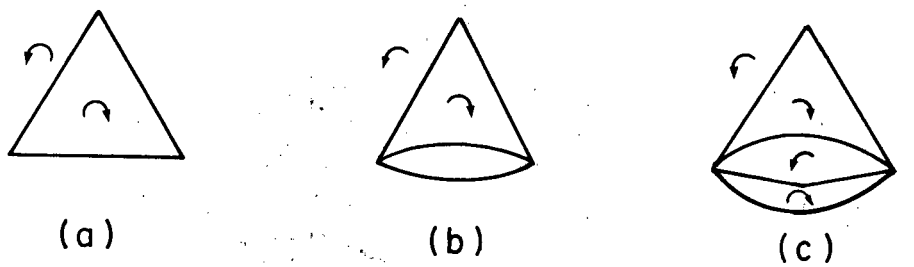

XBL 802-220

Figure 18

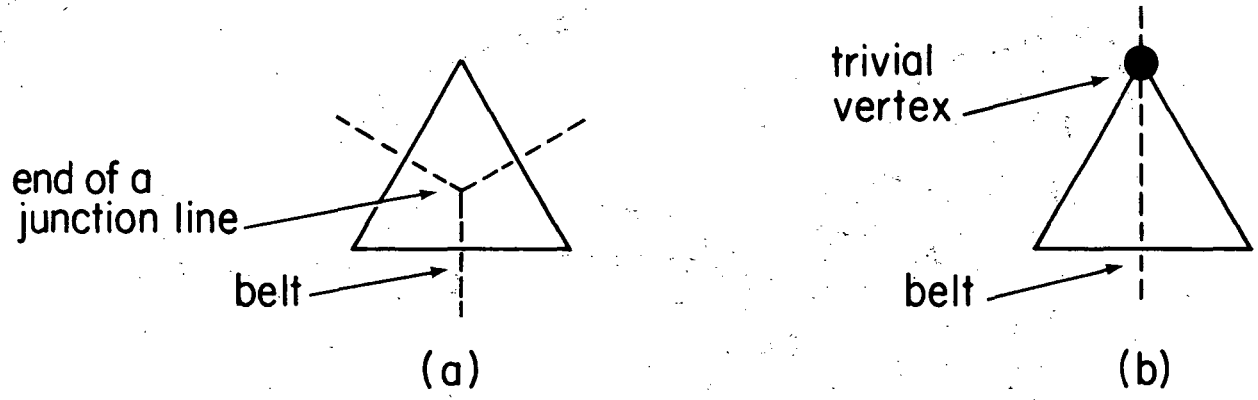

Figure 19

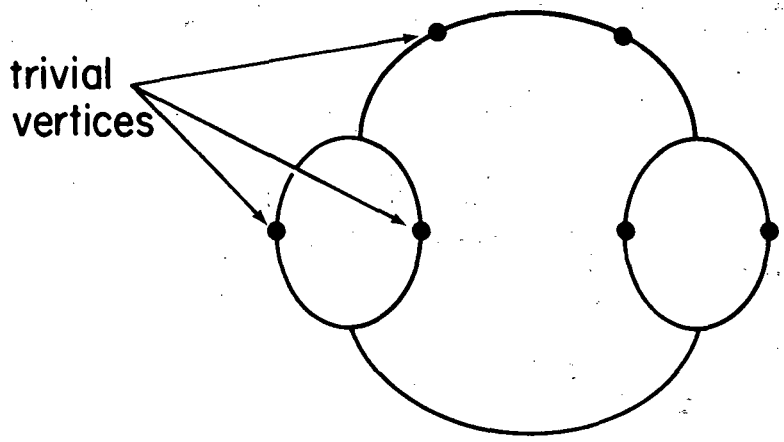

Figure 20

XBL 814-727

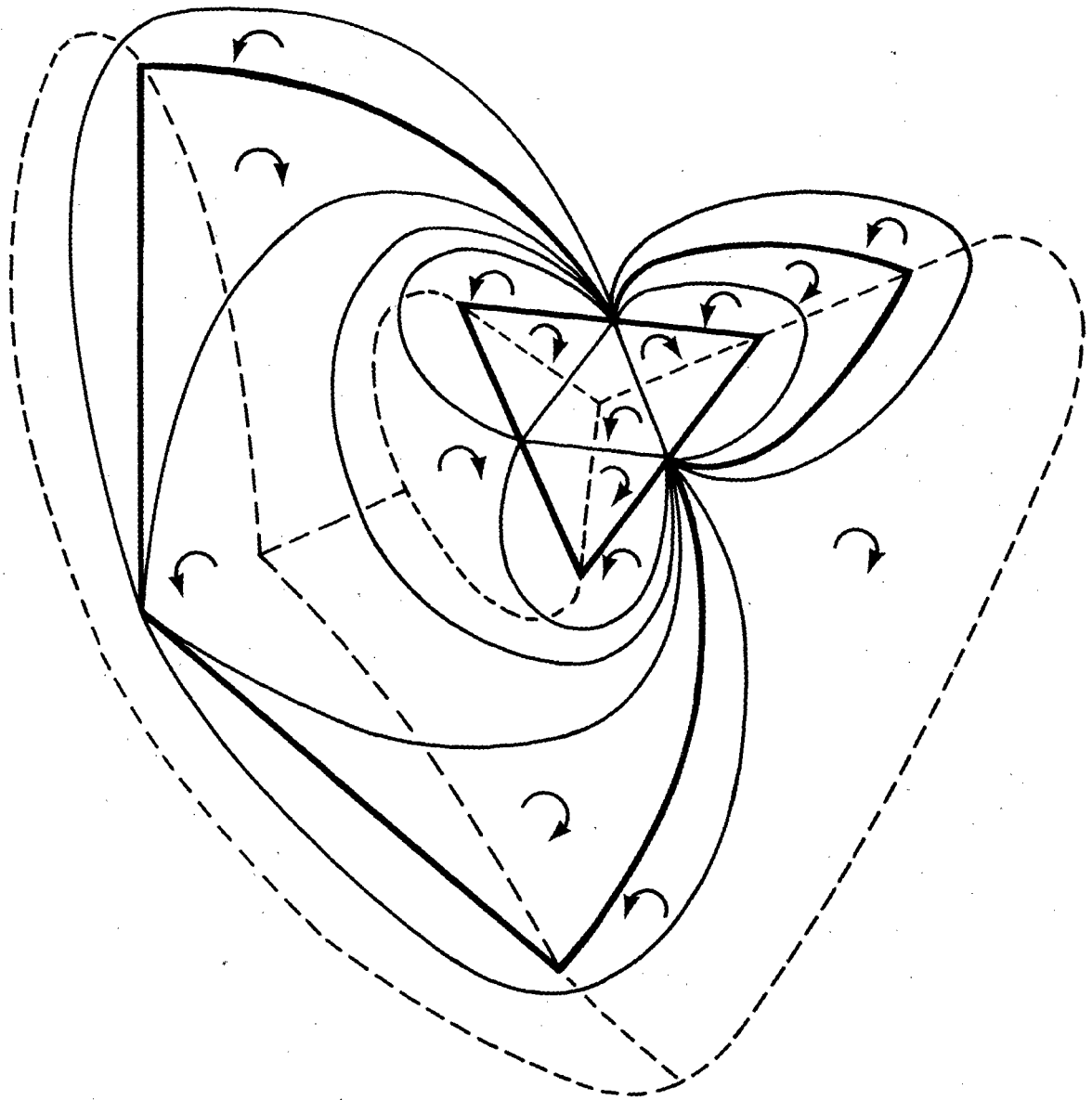

XBL 814-728

Figure 21

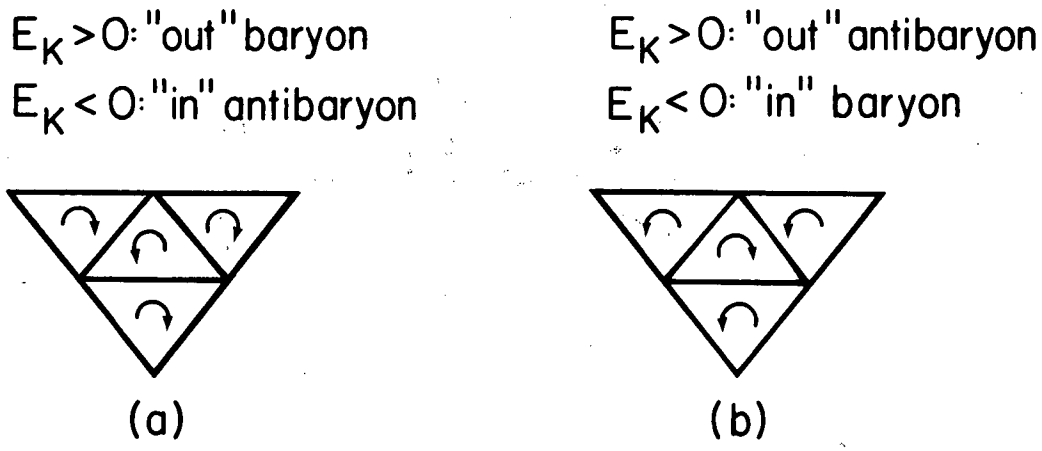

Figure 22

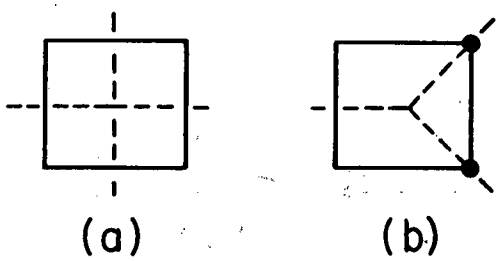

XBL 814-729

Figure 23

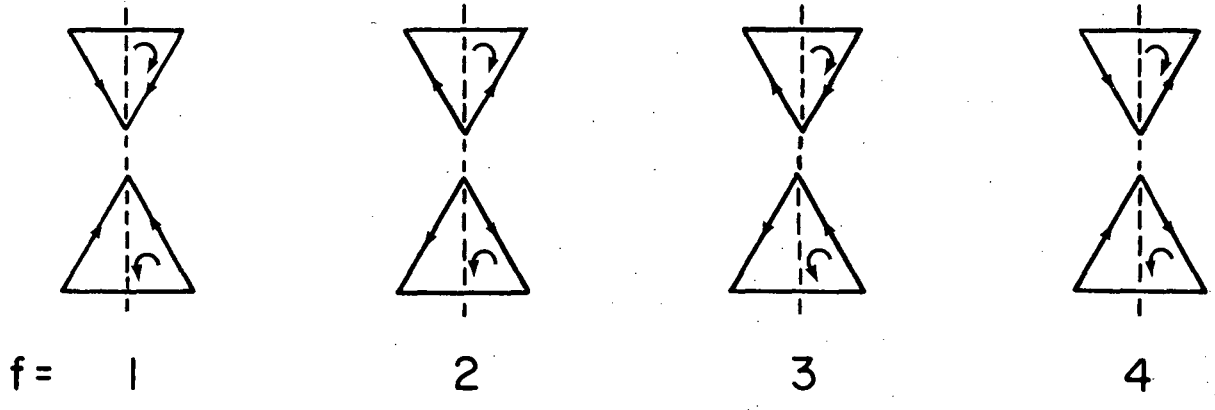

Figure 24

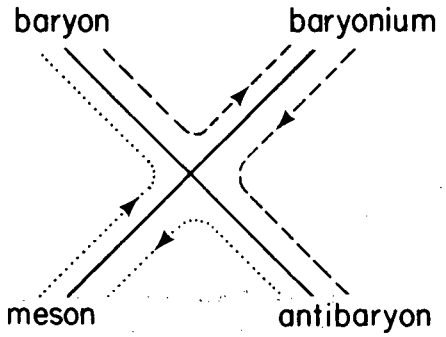

Figure 25

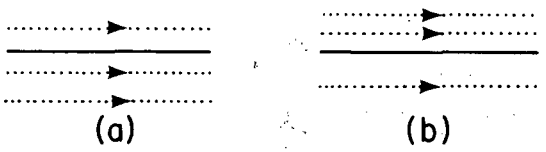

Figure 26

Figure 27

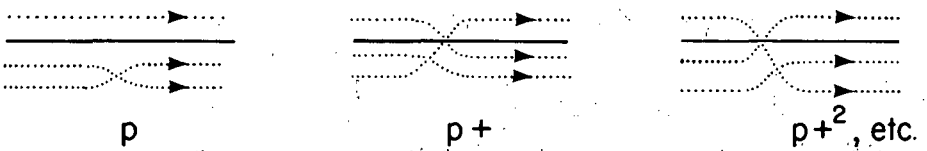

Figure 28

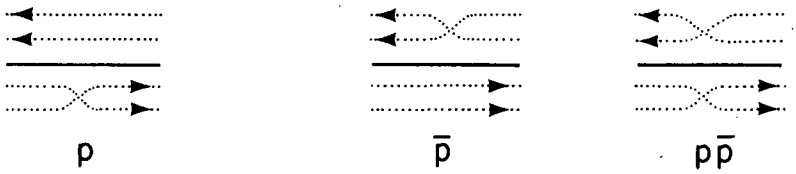

Figure 29

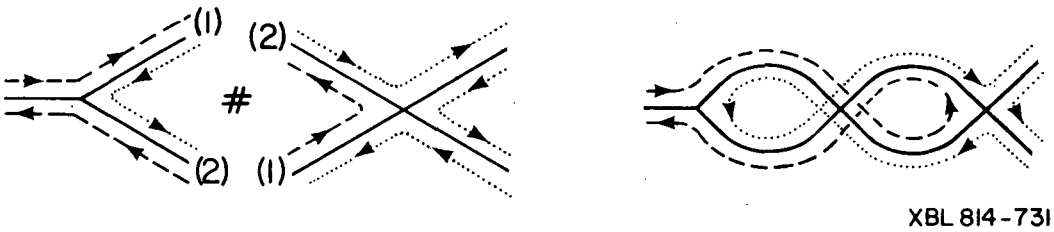

Figure 30

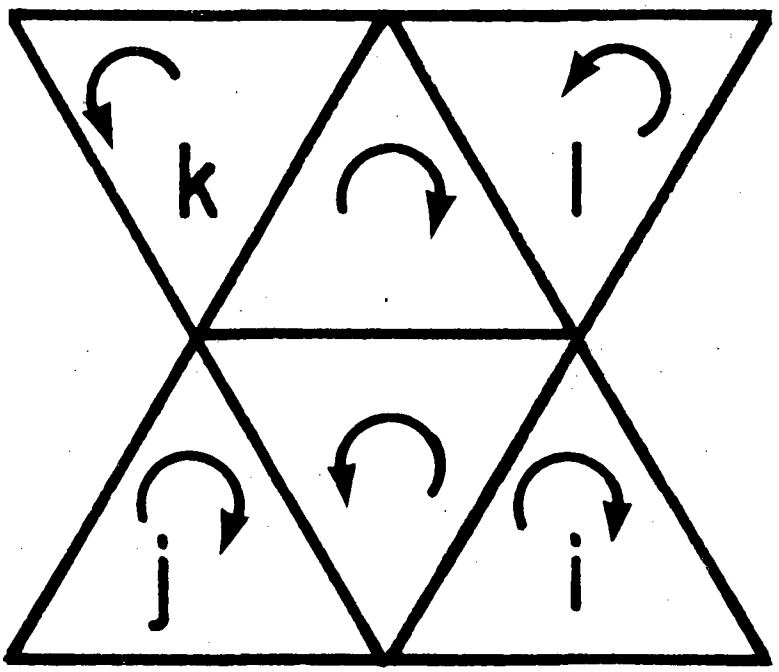

XBL 814-732

Figure 31

Figure 32

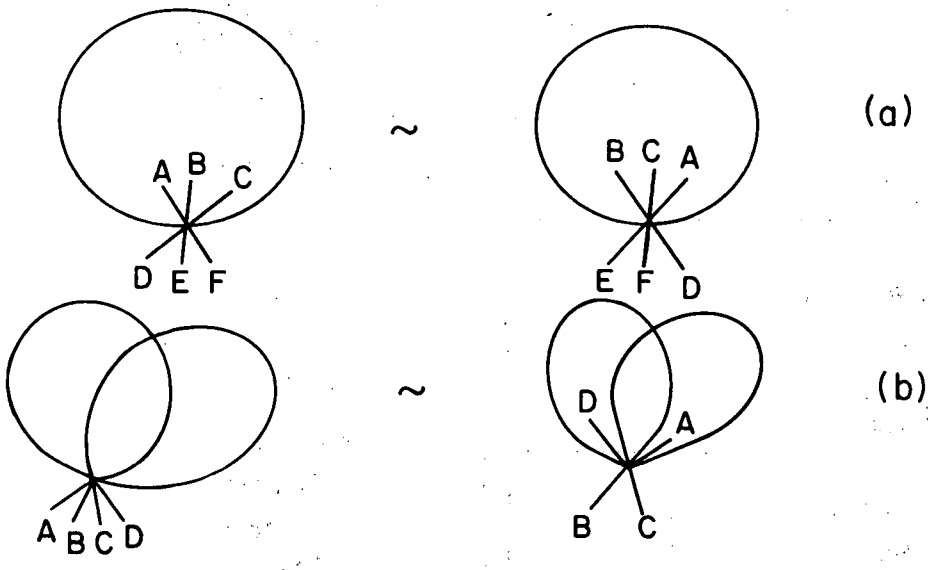

Figure 33

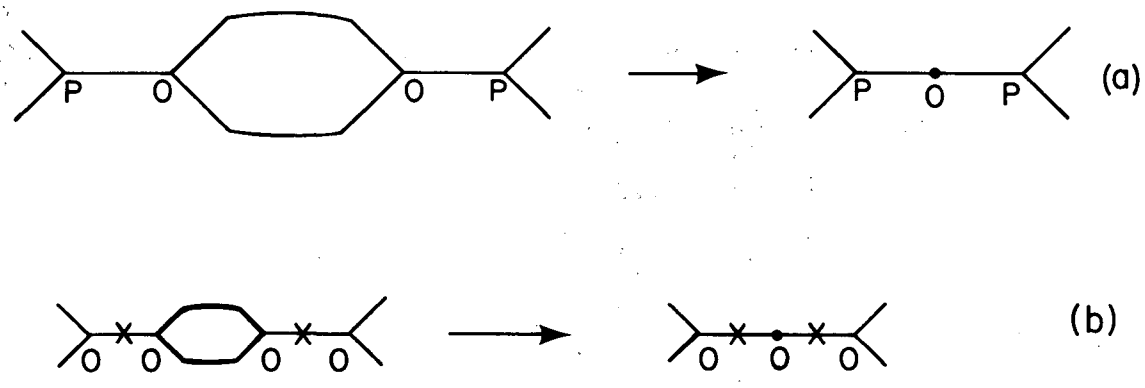

XBL 814-735

Figure 34

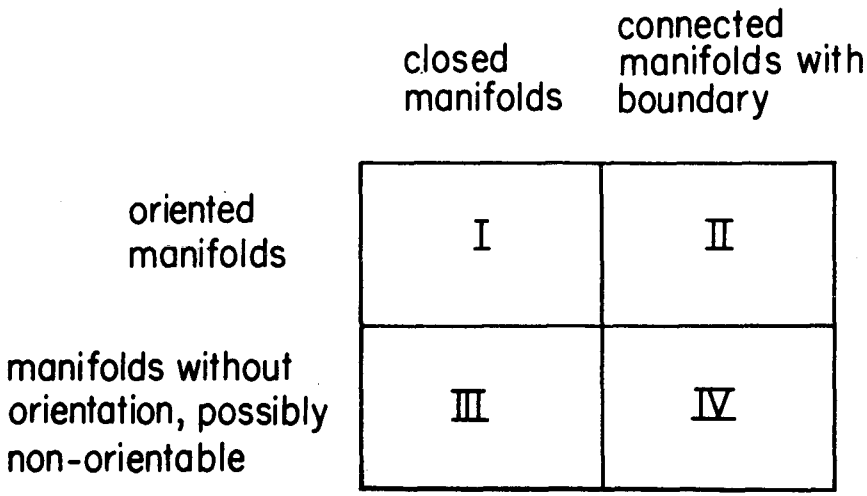

Figure 35

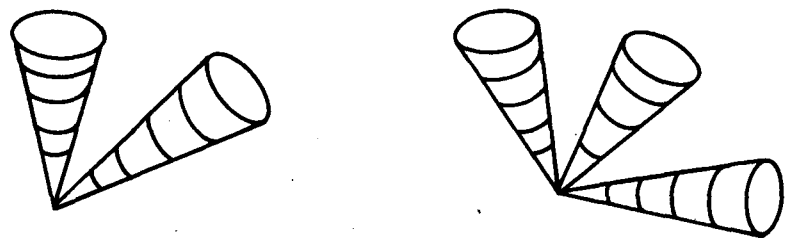

Figure 36

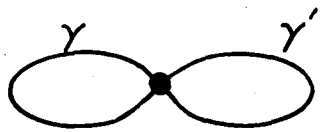

Figure 37

XBL 814-734

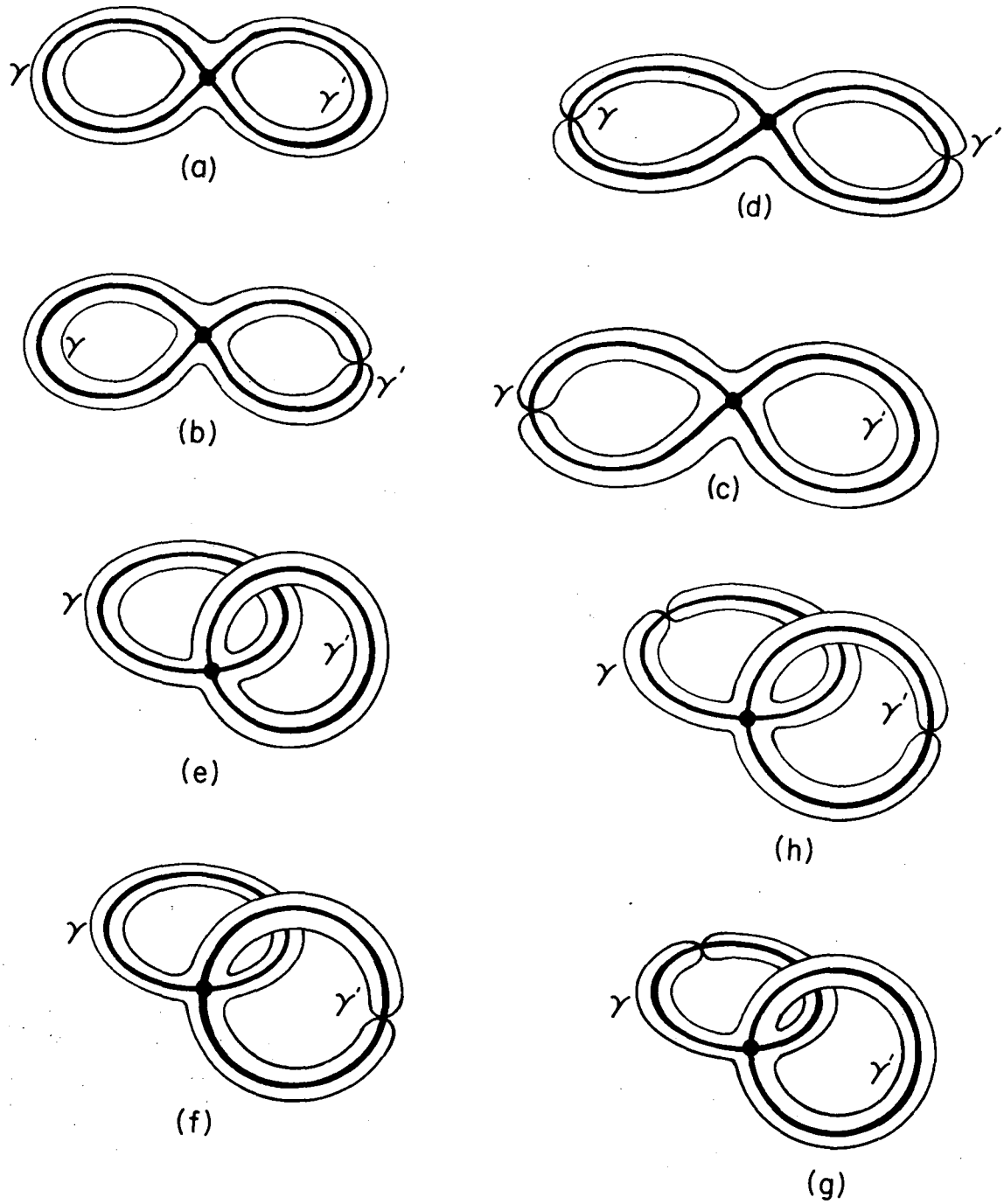

Figure 38

XBL 814-733

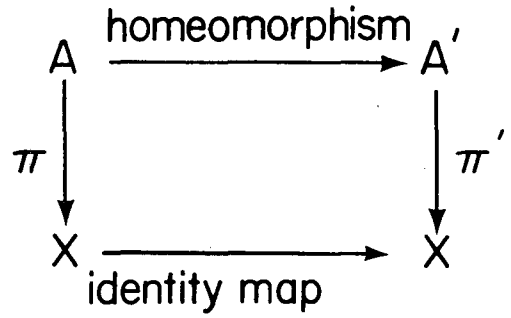

Figure 39

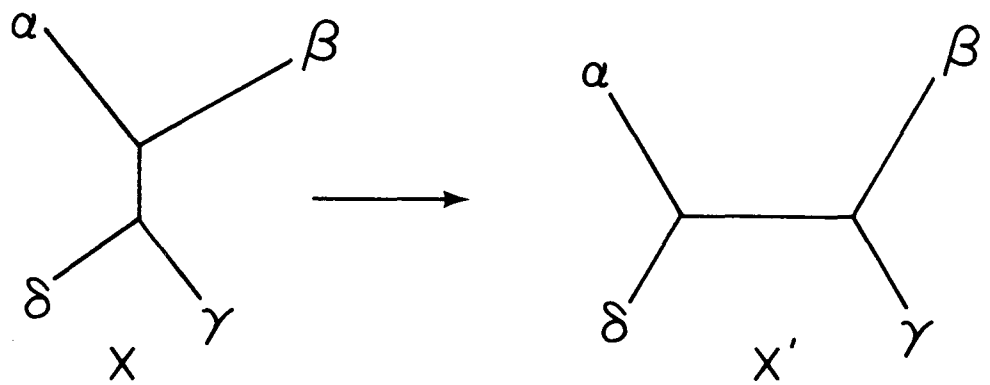

Figure 40

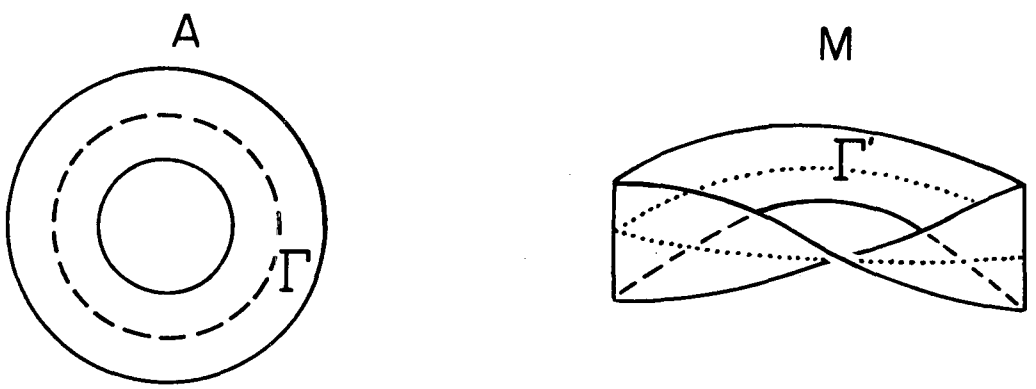

XBL 814-736

Figure 41

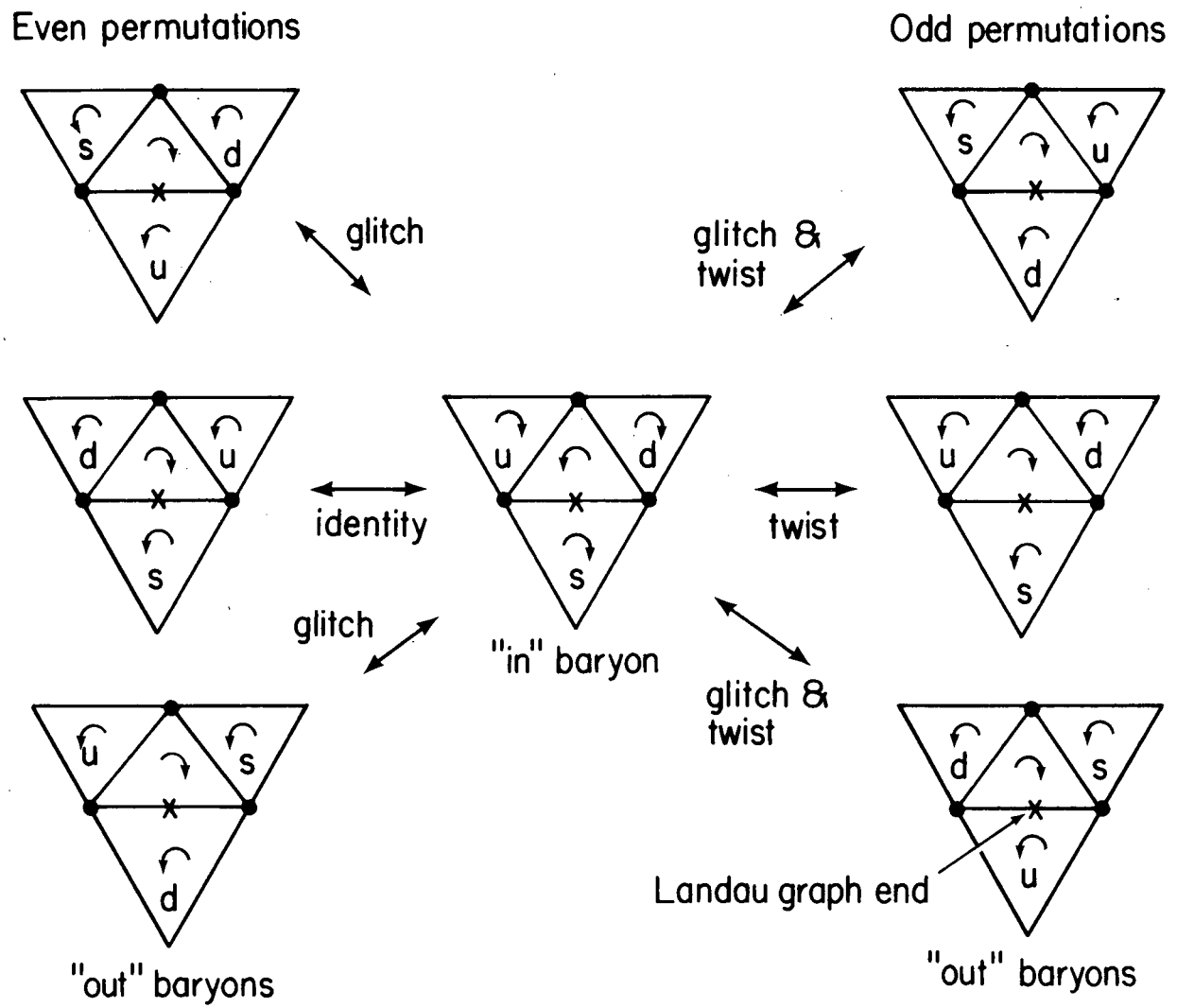

Figure 42

XBL 814-737

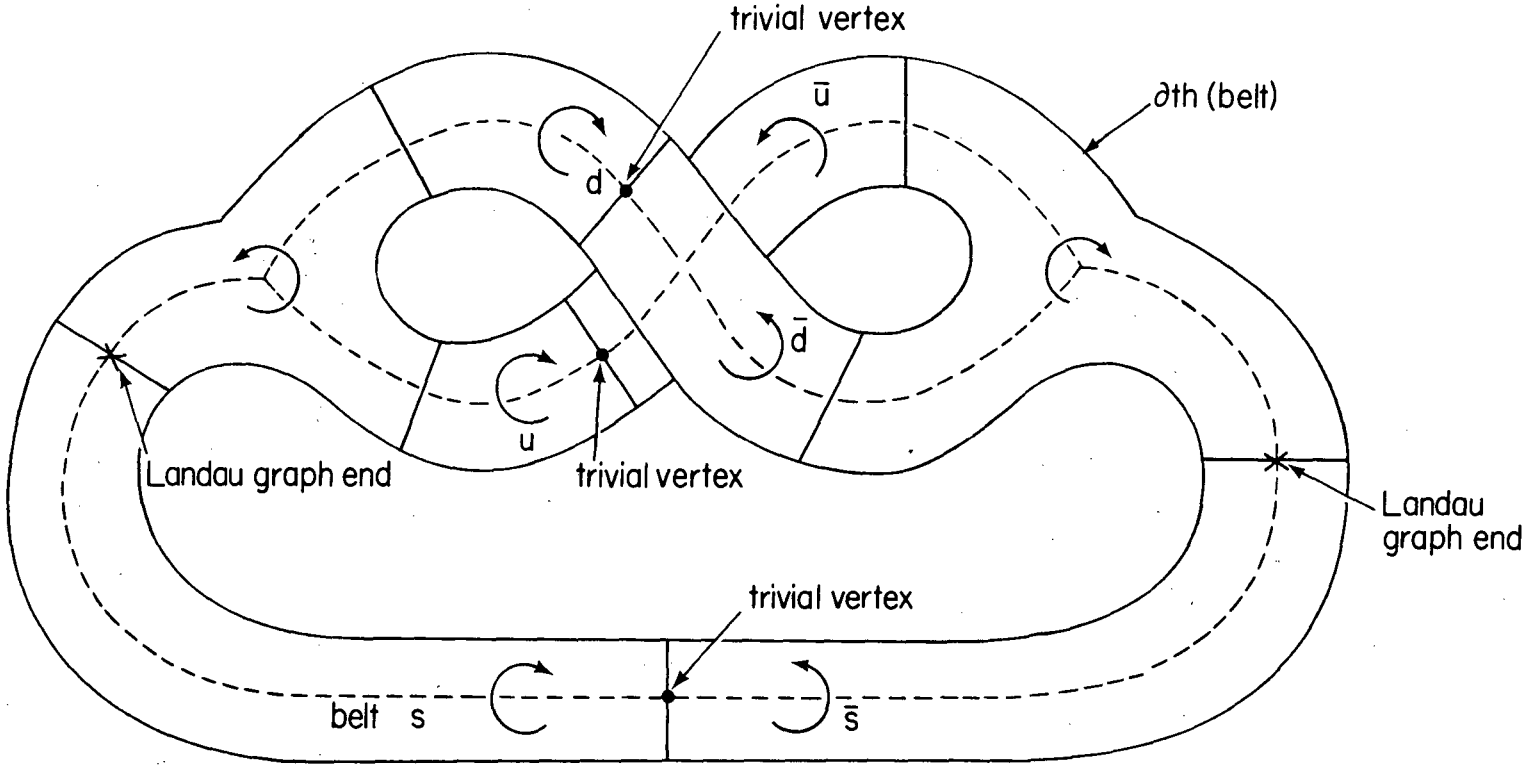

XBL 814-738

Figure 43

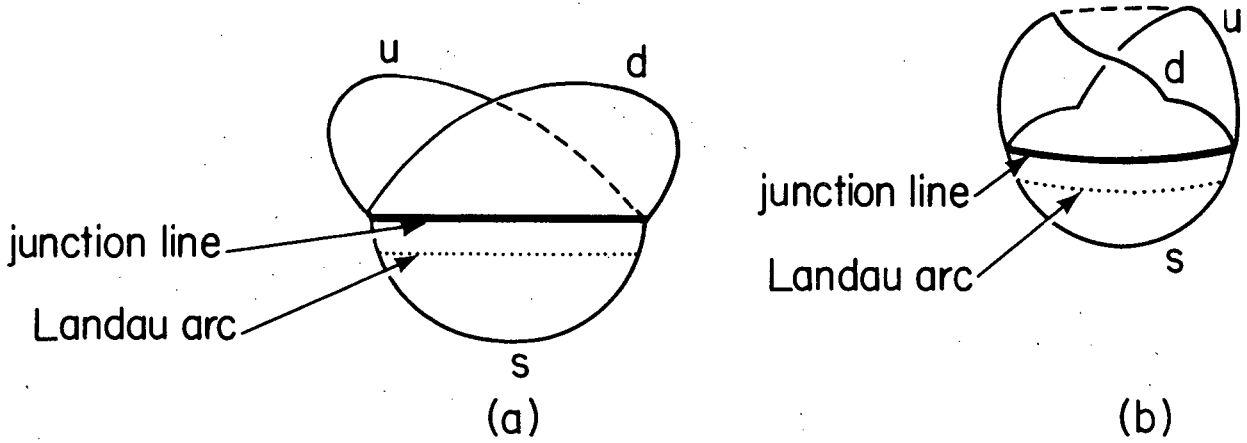

Figure 44

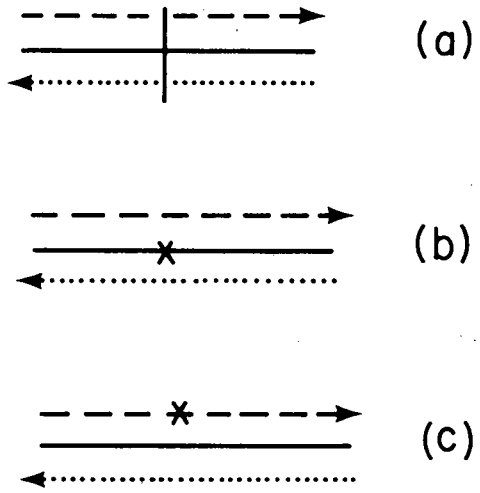

Figure 45

XBL 814-739

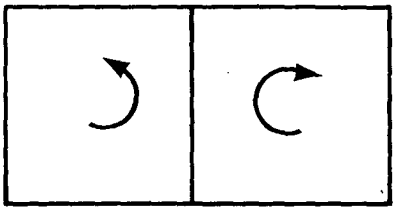

Figure 46

Figure 47

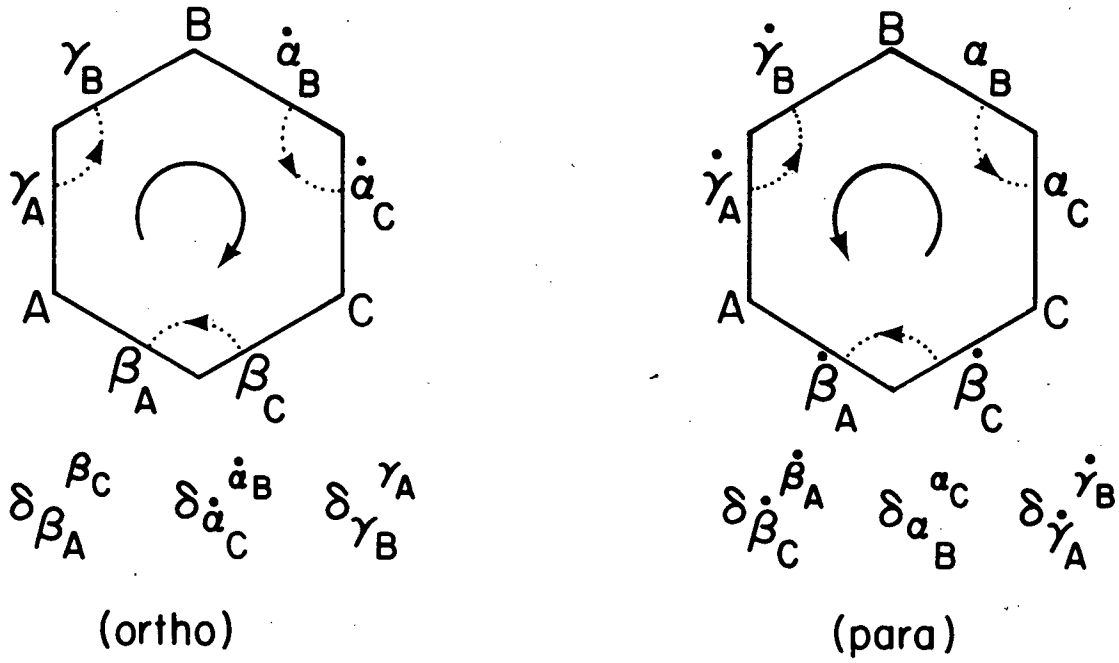

XBL 814-741

Figure 48

This report was done with support from the Department of Energy. Any conclusions or opinions expressed in this report represent solely those of the author(s) and not necessarily those of The Regents of the University of California, the Lawrence Berkeley Laboratory or the Department of Energy.

Reference to a company or product name does not imply approval or recommendation of the product by the University of California or the U.S. Department of Energy to the exclusion of others that may be suitable.

TECHNICAL INFORMATION DEPARTMENT
LAWRENCE BERKELEY LABORATORY
UNIVERSITY OF CALIFORNIA
BERKELEY, CALIFORNIA 94720